EPRI

2023 TECHNICAL UPDATE

Grid-Forming PV Inverter

Technology Development and Microgrid Applications

Grid-Forming PV Inverter

Technology Development and Microgrid Applications

3002028369

Technical Update, December 2023

EPRI Project Manager
W. Wang

EPRI
3420 Hillview Avenue, Palo Alto, California 94304-1338 USA
800.313.3774 ▪ 650.855.2121 ▪ askepri@epri.com ▪ www.epri.com

DISCLAIMER OF WARRANTIES AND LIMITATION OF LIABILITIES

THIS DOCUMENT WAS PREPARED BY THE ORGANIZATION(S) NAMED BELOW AS AN ACCOUNT OF WORK SPONSORED OR COSPONSORED BY THE ELECTRIC POWER RESEARCH INSTITUTE, INC. (EPRI). NEITHER EPRI, ANY MEMBER OF EPRI, ANY COSPONSOR, THE ORGANIZATION(S) BELOW, NOR ANY PERSON ACTING ON BEHALF OF ANY OF THEM:

(A) MAKES ANY WARRANTY OR REPRESENTATION WHATSOEVER, EXPRESS OR IMPLIED, (I) WITH RESPECT TO THE USE OF ANY INFORMATION, APPARATUS, METHOD, PROCESS, OR SIMILAR ITEM DISCLOSED IN THIS DOCUMENT, INCLUDING MERCHANTABILITY AND FITNESS FOR A PARTICULAR PURPOSE, OR (II) THAT SUCH USE DOES NOT INFRINGE ON OR INTERFERE WITH PRIVATELY OWNED RIGHTS, INCLUDING ANY PARTY'S INTELLECTUAL PROPERTY, OR (III) THAT THIS DOCUMENT IS SUITABLE TO ANY PARTICULAR USER'S CIRCUMSTANCE; OR

(B) ASSUMES RESPONSIBILITY FOR ANY DAMAGES OR OTHER LIABILITY WHATSOEVER (INCLUDING ANY CONSEQUENTIAL DAMAGES, EVEN IF EPRI OR ANY EPRI REPRESENTATIVE HAS BEEN ADVISED OF THE POSSIBILITY OF SUCH DAMAGES) RESULTING FROM YOUR SELECTION OR USE OF THIS DOCUMENT OR ANY INFORMATION, APPARATUS, METHOD, PROCESS, OR SIMILAR ITEM DISCLOSED IN THIS DOCUMENT.

REFERENCE HEREIN TO ANY SPECIFIC COMMERCIAL PRODUCT, PROCESS, OR SERVICE BY ITS TRADE NAME, TRADEMARK, MANUFACTURER, OR OTHERWISE, DOES NOT NECESSARILY CONSTITUTE OR IMPLY ITS ENDORSEMENT, RECOMMENDATION, OR FAVORING BY EPRI.

EPRI PREPARED THIS REPORT.

THIS REPORT WAS PREPARED AS AN ACCOUNT OF WORK SPONSORED BY AN AGENCY OF THE UNITED STATES GOVERNMENT. NEITHER THE UNITED STATES GOVERNMENT NOR ANY AGENCY THEREOF, NOR ANY OF THEIR EMPLOYEES, MAKES ANY WARRANTY, EXPRESS OR IMPLIED, OR ASSUMES ANY LEGAL LIABILITY OR RESPONSIBILITY FOR THE ACCURACY, COMPLETENESS, OR USEFULNESS OF ANY INFORMATION, APPARATUS, PRODUCT, OR PROCESS DISCLOSED, OR REPRESENTS THAT ITS USE WOULD NOT INFRINGE PRIVATELY OWNED RIGHTS. REFERENCE HEREIN TO ANY SPECIFIC COMMERCIAL PRODUCT, PROCESS, OR SERVICE BY TRADE NAME, TRADEMARK, MANUFACTURER, OR OTHERWISE DOES NOT NECESSARILY CONSTITUTE OR IMPLY ITS ENDORSEMENT, RECOMMENDATION, OR FAVORING BY THE UNITED STATES GOVERNMENT OR ANY AGENCY THEREOF. THE VIEWS AND OPINIONS OF AUTHORS EXPRESSED HEREIN DO NOT NECESSARILY STATE OR REFLECT THOSE OF THE UNITED STATES GOVERNMENT OR ANY AGENCY THEREOF

This is an EPRI Technical Update report. A Technical Update report is intended as an informal report of continuing research, a meeting, or a topical study. It is not a final EPRI technical report.

NOTE

For further information about EPRI, call the EPRI Customer Assistance Center at 800.313.3774 or e-mail askepri@epri.com.

Together…Shaping the Future of Energy®

© 2023 Electric Power Research Institute (EPRI), Inc. All rights reserved. Electric Power Research Institute, EPRI, and TOGETHER…SHAPING THE FUTURE OF ENERGY are registered marks of the Electric Power Research Institute, Inc. in the U.S. and worldwide.

ACKNOWLEDGMENTS

The following organizations prepared this report:

EPRI

Principal Investigators
W. Wang
T. Kim
J. Baum
A. Renjit

University of Wisconsin-Madison

Principal Investigators
D. Gross
A. Afshari

This report describes research sponsored by EPRI.

This material is based upon work supported by the U.S. Department of Energy's Office of Energy Efficiency and Renewable Energy (EERE) under the Solar Energy Technologies Office Award Number DE-EE0009336.

This publication is a corporate document that should be cited in the literature in the following manner: *Grid-Forming PV Inverter: Technology Development and Microgrid Applications.* EPRI, Palo Alto, CA: 2023. 3002028369.

ABSTRACT

Presently, excluding residential backup power applications, grid-forming (GFM) inverters are commercially available for battery energy storage system (BESS) and some PV plus battery systems but not yet for stand-alone PV. This tech update investigates the control design for GFM PV inverter, especially the control required to provide active power reserve and to stabilize the dc link voltage.

Subsequently, the use cases of GFM PV plants in utility-level microgrids are discussed considering fully inverter-based microgrids (i.e., with PV and BESS) as well as mixed-source microgrids (i.e., with PV and diesel generator). Scenarios where active power up-reserve from GFM PV plants is beneficial are illustrated. Moreover, requirements and specifications for GFM PV plant, especially for its active power reserve function are developed.

In addition, stability of an example utility-level microgrid with two GFM PV plants and a diesel generator is analyzed to shed light on the potential unstable interaction between multiple GFM resources and the countermeasures.

This research aims to advance GFM PV technology to offer more flexibility in microgrid design. With GFM PV available, depending on the level of reliability required, cost-benefit analysis, etc., the GFM BESS or diesel generator may be sized smaller while leveraging the full potential of PV generation inside the microgrid.

Keywords

DER, grid-forming, microgrid, power reserve, solar PV, stability

CONTENTS

1 Introduction 1

2 Control Design for Grid-Forming PV Inverter 4

Overall Control Structure 4

Active Power Limiting and DC Voltage Control 6

Maximum Power Point Estimation 8

3 Use Cases of Grid-Forming PV Plants in Microgrids 10

Active Power Reserve from GFM PV Plants 10

Use Case of GFM PV Active Power Reserve in Fully Inverter-Based Microgrids 13

Use Case of GFM PV Active Power Reserve in Microgrids with Slower-Response Resources 15

General Use Cases 16

Use case to support unbalanced load and maintain voltage balance 17

Use case to support nonlinear load and restrict voltage harmonics 17

Use case to black start the microgrid 18

4 Requirements and Specifications for GFM PV Plants Active Power Reserve Function 20

Requirements and Specifications in Fully Inverter-Based Microgrids 20

Steady state requirements 21

Dynamic/transient requirements 23

Simulation demonstration 27

Requirements and Specifications in Microgrids with Slower-Response Resources 30

Steady state requirements 30

Dynamic/transient requirements 31

Simulation-based setting guideline and demonstration 36

5 Stability Analysis in Microgrids with GFM PV and Diesel Generator 39

Stability Criteria 39

Microgrid Stability with Different GFM PV and Diesel Generator Control Settings 40

Considerations in maintaining PV dc voltage stability 40
Stable regions in the parameter space 42
Simulation Demonstration 44
PV dc bus voltage instability 44
Instability caused by overloading the generation resources 46
Instability under low solar irradiance scenarios 47

6 Conclusion and Future Work 50

LIST OF FIGURES

Figure 1. Illustration of a utility-level microgrid with one GFM BESS and multiple GFL PV plants 2
Figure 2. Illustration of a utility-level microgrid with high PV-to-BESS capacity ratio by utilizing GFM PV 3
Figure 3. Block diagram of the PV plant and its GFM inverter control 5
Figure 4. Detailed control implementation in P-f, Q-V, and current controls 5
Figure 5. Stable and unstable dc bus voltage regions with a particular irradiance and temperature 6
Figure 6. Detailed implementation of dc voltage control 7
Figure 7. Example P-f droop curves on a GFM PV inverter and a diesel generator to show power sharing 8
Figure 8. Single-diode equivalent circuit of PV panels 9
Figure 9. Verification of the implemented MPP estimation method 9
Figure 10. Two control methods to realize up-reserve in GFM PV plants 11
Figure 11. Response comparison between the two APR methods 12
Figure 12. Hierarchical control of DER in a microgrid including APR for GFM PV 13
Figure 13. Operation Scenarios in a fully GFM inverter-based microgrid with PV and BESS with PV net load along the horizontal axis. Scenarios: a) load must be curtailed, b) BESS must discharge, c) BESS can charge, and d) PV must be curtailed. 14
Figure 14. Example mixed-source microgrid based on modified IEEE 13 bus feeder 16
Figure 15. Comparison of active power and frequency responses without PV APR (case 1) vs with PV APR (case 2) 16
Figure 16. P-f droop settings for PV and BESS plants when SoC of the BESS is low 21
Figure 17. P-f droop settings for PV and BESS plants when SoC of the BESS is high 22
Figure 18. P-f droop settings for PV and BESS plants when SoC of the BESS is 100% 23
Figure 19. Illustration of the allowed frequency region following the specified disturbances 24
Figure 20. Example fully inverter-based microgrid based on modified IEEE 13 bus feeder 28
Figure 21. Response from PV and BESS following the load step increase 29
Figure 22. Response from PV and BESS following the load step decrease 29
Figure 23. Response from PV and BESS following the irradiance decrease 30
Figure 24. The proposed P-f droop setting approach for PV and SG plants 31
Figure 25. Frequency nadir for various M/TT ratios and effective droop gains $Kdr + k = 1Nmp, k - 1$ for a 1 p.u. load step 34

Figure 26. Frequency nadir for different (reference) governor gains Kdr, aggregate inverter droop gains $k = 1Nmp, k - 1$, and $M/TT = 10$ 35
Figure 27. Illustration of the simulation-based slope setting approach 37
Figure 28. Verification of the droop setting approach with consecutive load changes 38
Figure 29. Verification of the droop setting approach with change in initial operating condition 38
Figure 30. Example P-V characteristics for different levels of irradiance 41
Figure 31. Stability regions for 1%-20% device based droop ranges 43
Figure 32. Stability regions for different levels of irradiance 44
Figure 33. Instability caused by the dc voltage drop when the dc voltage limit is set to 1020V in the dc voltage controller 45
Figure 34. System recovered from dc voltage drop when the dc voltage limit is set to 1040V in the dc voltage controller 46
Figure 35. Stable system with sufficient headroom to cover load increase 47
Figure 36. Instability caused by the saturation of all generation resources 47
Figure 37. Small-signal instability caused by choosing inappropriate dc voltage limit 48
Figure 38. System recovered by increasing the dc voltage limit 48
Figure 39. Large-signal instability caused by low frequency droop gain at low irradiance levels 49
Figure 40. Stable system with high frequency droop gains at low irradiance levels 49

LIST OF TABLES

Table 1. Operation modes of PV, BESS and load corresponding to different scenarios 14

1 INTRODUCTION

Microgrid implementation, often called intentional islanding, is an effective way to improve resilience of a section of power distribution grid. Among the different scales of microgrids, utility-level multi-customer microgrid which involves utility medium voltage (MV) feeder and loads/generation(s) at different locations, is of particular interest to utility operators. A number of pilot feeder-level microgrids are already set up and running at different locations across the US and around the world[1].

Traditionally, microgrids have been designed with diesel generators as the main generation resources. With the increasing penetration of inverter-based distributed energy resources (DERs), such as solar photovoltaic (PV) and battery energy storage system (BESS), there is also a growing interest to design fully inverter-based microgrids. However, present-day inverter control technologies are mainly designed to operate in the presence of (or parallel with) a stiff power system, which are often termed as "grid-following (GFL) inverter control". Such inverter control approaches face challenges to provide grid services and maintain stability in inverter-dominated systems, such as in a fully inverter-based microgrid[1].

To deal with the challenges, improvement of the present-day control design and various new forms of inverter controls have been proposed. These controls are termed as "grid forming (GFM) inverter control" due to their capability to form grid voltage and operate without relying on synchronous machines[1]. Presently, excluding residential backup power applications, GFM inverters are commercially available for battery energy storage system (BESS) and some PV plus battery systems but not yet for stand-alone PV. Similar to a diesel generator, a GFM BESS can be utilized as the master of a microgrid.

In today's utility-level microgrid design, the capacity of the GFM DERs (typically BESS or diesel generator) is often selected large enough to supply the entire microgrid loads during islanded operation. Moreover, the GFL DERs (e.g., behind-the-meter or utility-scale PV) inside the microgrid footprint may be required to be offline during the microgrid islanded operation due to the concern that they may jeopardize the microgrid stability and/or power quality, especially when the aggregated capacity of the GFL DERs is similar to or greater than that of the GFM DERs.

However, there is a clear benefit of operating the existing GFL PV plants in parallel with the GFM BESS or diesel plant(s), as they can help supply the load and hence may reduce the size (kW and kWh) and cost of the BESS or diesel generator. Moreover, the BESS may be charged during times with excess PV generation, such that the microgrid can operate longer, thereby further increasing grid resilience. An illustration of a utility-level microgrid with a GFM BESS and multiple GFL PV plants is shown in Figure 1.

[1] *Grid Forming Inverters: EPRI Tutorial (2023).* EPRI, Palo Alto, CA: 2023. 3002028090.

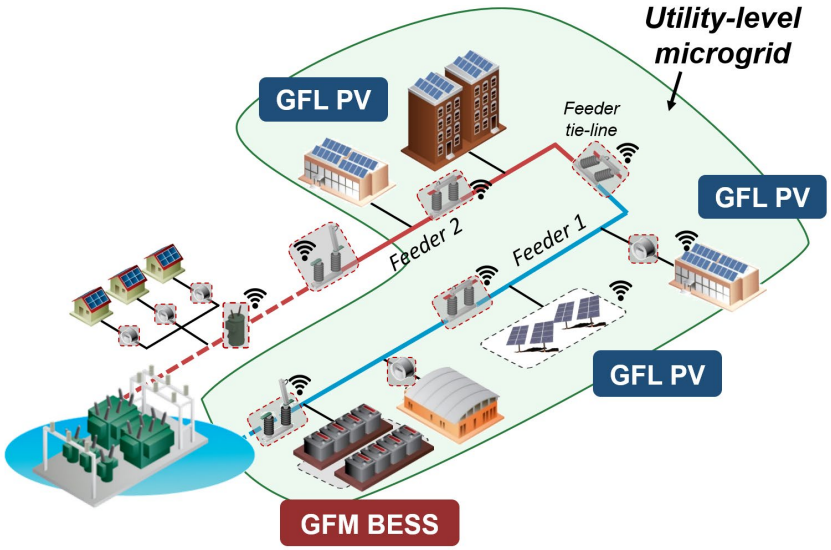


Figure 1. Illustration of a utility-level microgrid with one GFM BESS and multiple GFL PV plants

The possibility of operating GFL PV plants together with GFM BESS in a utility-level microgrid has been investigated[2,3]. Results show that active islanding detection from GFL PV plants may cause sustained voltage and frequency oscillations in the microgrid hence creating power quality concerns. Moreover, even if active islanding detection is disabled on the GFL plants, the GFL-to-GFM capacity ratio must be limited (e.g., the GFL DER capacity cannot be higher than 1.5 times of the GFM DER capacity in certain cases) to avoid transient instability of the GFL plants following large disturbances.

Since the GFL-to-GFM DER capacity ratio needs to be limited to ensure microgrid stability, to enable microgrids with high PV-to-BESS or PV-to-diesel generator capacity ratio, it is worth exploring operating some of the PV plants in GFM mode. Unlike GFL PV, it is expected that GFM PV plants could contribute positively to microgrid voltage and frequency regulation and help maintain microgrid stability and power quality. A microgrid design with high PV-to-BESS capacity ratio is illustrated in Figure 2, where the size of the GFM BESS can be smaller compared to that in Figure 1 due to operating two of the PV plants in GFM mode.

Since GFM PV inverter is not commercially available, its control strategy needs to be devised. One unique feature of GFM PV plant is that it should be able to provide active power up-reserve or headroom when needed. When providing up-reserve, PV is not working at maximum power point and today's maximum power point tracking methods no longer work. Therefore, a method to estimate the maximum power point is required. Moreover, since the voltage of PV

[2] *Impact of Active Islanding Detection on Microgrid Voltage and Frequency.* EPRI, Palo Alto, CA: 2023. 3002028374.

[3] *Performance Requirements for Grid Forming Inverter Based Power Plant in Microgrid Applications: Second Edition.* EPRI, Palo Alto, CA: 2022. 3002024431.

panels is less stiff than a battery, proper control design is required to avoid the dc voltage collapse during dynamic conditions.

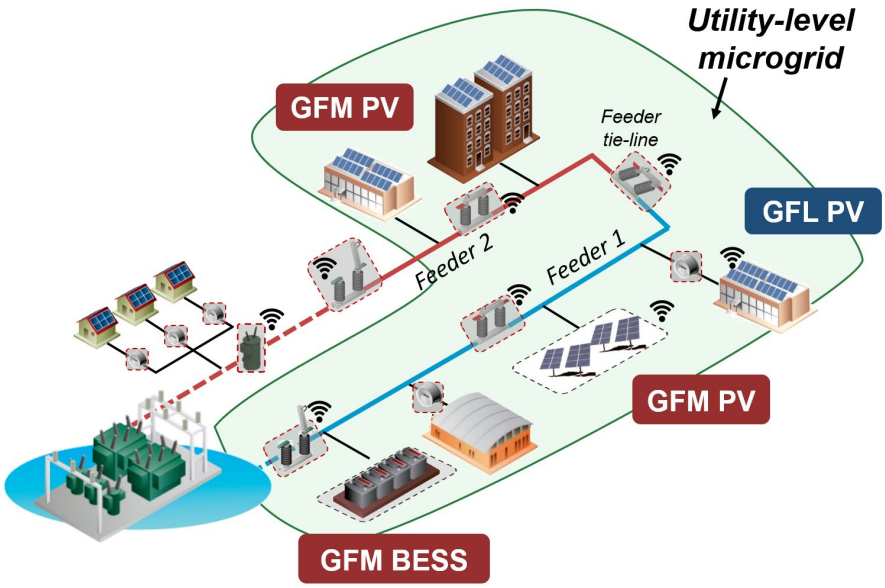


Figure 2. Illustration of a utility-level microgrid with high PV-to-BESS capacity ratio by utilizing GFM PV

The DOE Solar Energy CommUnity REsilience (SECURE) project led by EPRI aims at addressing the key technical and business challenges impeding implementation of resilient community microgrids. Key components of the research include de-centralized autonomous community control, islandable communication systems, viable economic frameworks for community microgrids, and advancement in GFM PV inverter capability to address microgrid stability issues with high PV penetration (above 80% of the total generation capacity).

This tech update presents available results from the ongoing DOE SECURE project in the aspects of GFM PV inverter control design, its use cases in microgrid applications, and its performance requirements and specifications. Moreover, stability of an example microgrid with two GFM PV plants and a diesel generator is analyzed to shed light on the potential unstable interaction between multiple GFM resources and the countermeasures.

It should be emphasized that due to the intermittent nature of PV available power, a microgrid dominated by PV generation has clear pros and cons. The advantage is that it can reduce the cost of BESS or diesel generator and may enable temporary microgrid operation even when the BESS/diesel generator is not available. However, it is less reliable and could trigger load shedding or shut-down of the microgrid when PV available power is low. Besides, it may not be able to support the microgrid operation during nighttime. Therefore, GFM PV is not to replace GFM BESS or diesel generator but to offer more flexibility in microgrid design. Depending on the level of reliability required, cost-benefit analysis, etc., the GFM BESS/diesel generator could be sized smaller while leveraging the full potential of PV generation inside the microgrid.

2 CONTROL DESIGN FOR GRID-FORMING PV INVERTER

Compared to battery energy storage, the voltage at the terminal of the PV panel is less stiff and varies with PV irradiance, temperature, and PV output current/power. When designing grid-forming control for PV, extra care should be taken to ensure proper voltage regulation at the dc bus and avoid the potential risk of dc voltage collapse. In a single-stage design without a dc-to-dc converter, the voltage at the dc bus is the same as the PV panel terminal voltage and varies with operating conditions. In this case, it is especially important that the inverter control can limit its active power output whenever needed to prevent dc voltage collapse. Moreover, due to the dependency on solar irradiance and temperature, the maximum available power of PV is not firm but time varying. Therefore, when designing active power reserve for GFM PV, a method to estimate the maximum power point (MPP) is required.

These two aspects are quite unique to GFM PV inverters and one way to design the inverter control to achieve these is detailed in this chapter. Besides, the overall control structure and the control components that can also apply to GFM BESS inverters are introduced. In this project, the GFM inverter control is implemented and tested in MATLAB/Simulink.

Overall Control Structure

Figure 3 shows the physical and control structure of the GFM PV plant. The dc side has a single-stage design where the PV panels are directly connected to the dc link capacitor without a dc-to-dc converter. Such a design saves cost on the converter but puts higher requirement on the inverter control to maintain stability of the dc link voltage.

The active power-frequency (P-f) control implements a droop characteristic between the inverter active power output and the frequency it generates. Similarly, a droop characteristic between the inverter reactive power output and its terminal voltage is established by the reactive power-voltage (Q-v) control. The P-f and Q-V control determine the angle and voltage references of the inverter output which are passed onto the virtual impedance and current limiting control where the output current references are calculated and limited. Following that, current control makes sure that the output current from the inverter follows the reference by adjusting the voltage generated at the power electronic switches. Detailed control implementations inside these blocks are shown in Figure 4. The various PI control parameters and virtual impedance values should be properly tuned and may not be changed by a user. The main parameters that a user needs to specify include the active power reference P_{ref} (when system frequency is at nominal, e.g., 60 Hz), voltage reference V_{ref} (when inverter output reactive power is zero), and the P-f and Q-v droop gains D_p and D_q. More details of these controls can be found in literature[4].

[4] X. Quan et al., "Photovoltaic Synchronous Generator (PVSG): Architecture and Control Strategy for A Grid-Forming PV Energy System," in IEEE Journal of Emerging and Selected Topics in Power Electronics, June 2020.

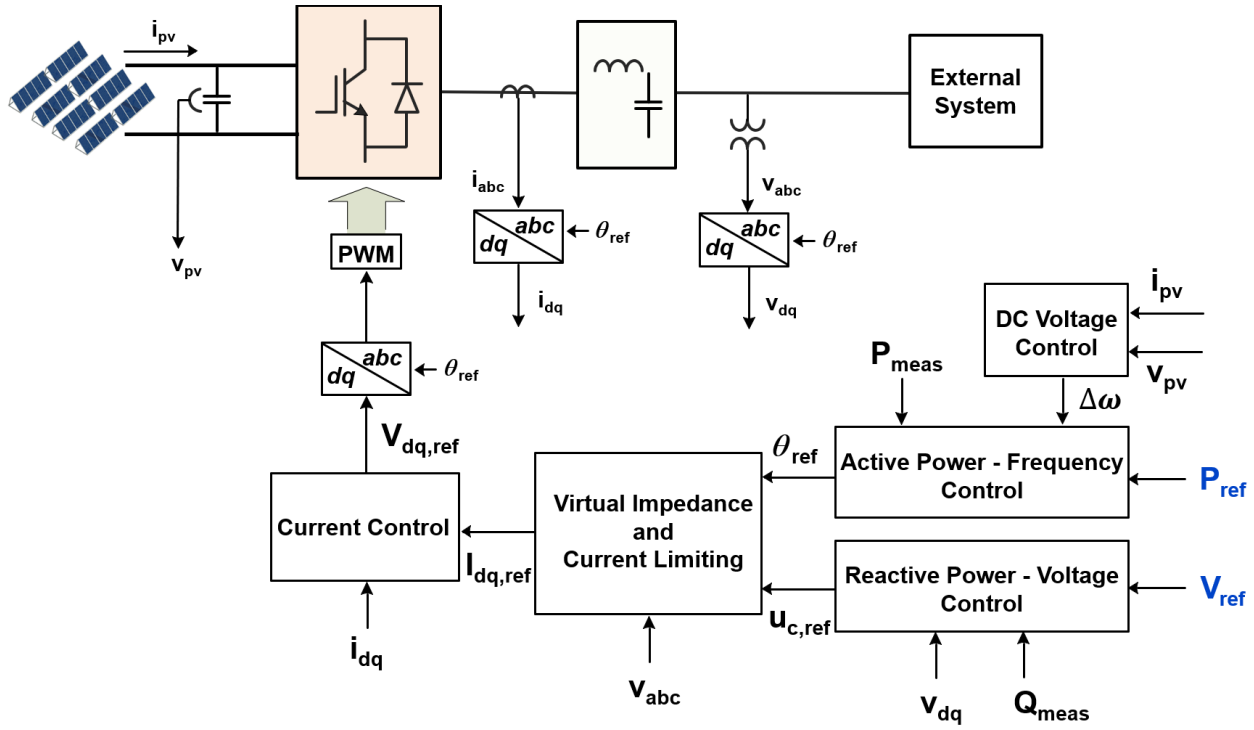


Figure 3. Block diagram of the PV plant and its GFM inverter control

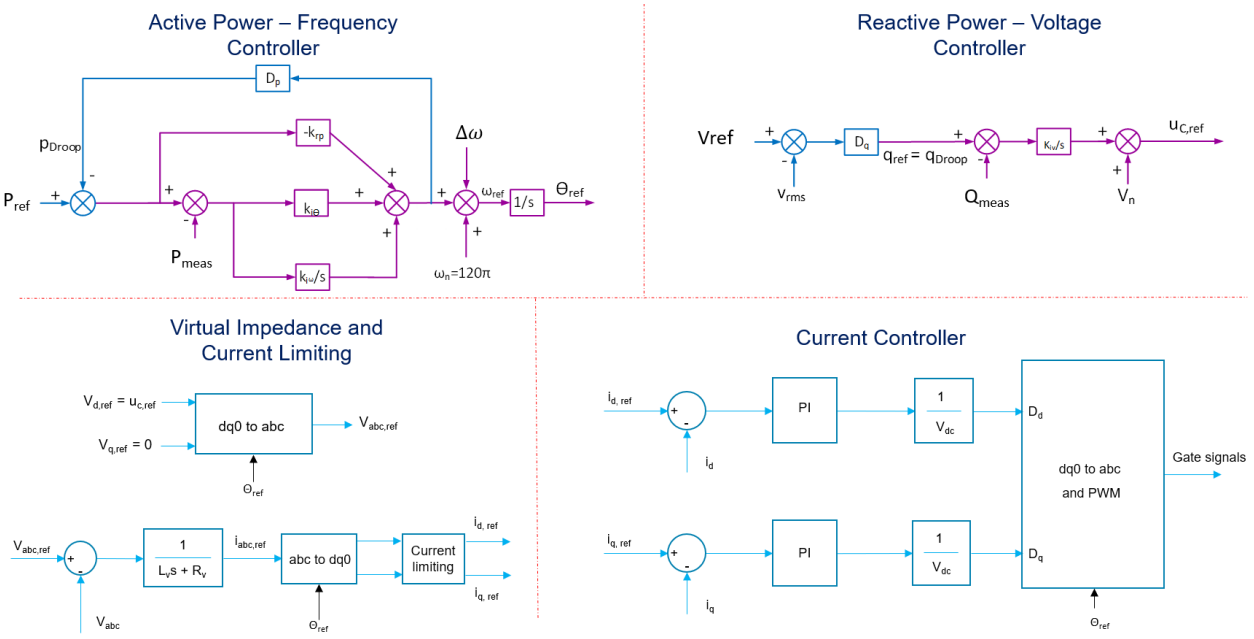


Figure 4. Detailed control implementation in P-f, Q-V, and current controls

These control blocks can be applied to other GFM technologies such as GFM BESS. The dc voltage control block which includes the MPP estimation is unique to GFM PV inverter and is illustrated in detail next.

Active Power Limiting and DC Voltage Control

In the single-stage design shown in Figure 3, ignoring the inverter losses, the active power output from the PV panels is directly related to the dc bus voltage. An example relationship given a particular solar irradiance level and temperature is shown in Figure 5. The dc bus voltage that corresponds to the MPP (V_{mpp}) is 1000V in this case whereas the open circuit voltage is 1200V. When the dc bus voltage is between 1000V and 1200V, an increase in inverter ac active power output causes dc bus voltage to decrease which then causes more output power from the PV panel to match the ac output and avoid further dc voltage decrease. Therefore, when operating inside this region, the PV panel provides stabilizing impact on dc bus voltage and the region is termed as stable region. In contrast, when operating below 1000V, a decrease in dc voltage causes the output power from the PV panel to reduce, which further reduces the dc bus voltage. It is therefore termed as unstable region.

When operating in GFM mode, the PV plant follows the load changes inside the microgrid. There can be situations where a load increase causes the GFM PV inverter to output power higher than its MPP during the dynamic time frame. For example, consider a microgrid with one GFM PV plant and one BESS and the PV plant is working at MPP initially. When a sudden load increase occurs, the GFM PV will output power higher than its MPP trying to balance the load. In this case, the dc bus voltage will decrease and can go inside the unstable region. The GFM PV inverter control should react quickly to reduce its active power output and bring the dc bus voltage back to the stable region before it collapses, which is the goal of the dc voltage control. With proper dc voltage control, the GFM PV output in this example can be limited at the MPP while the load increase is picked up by the BESS.

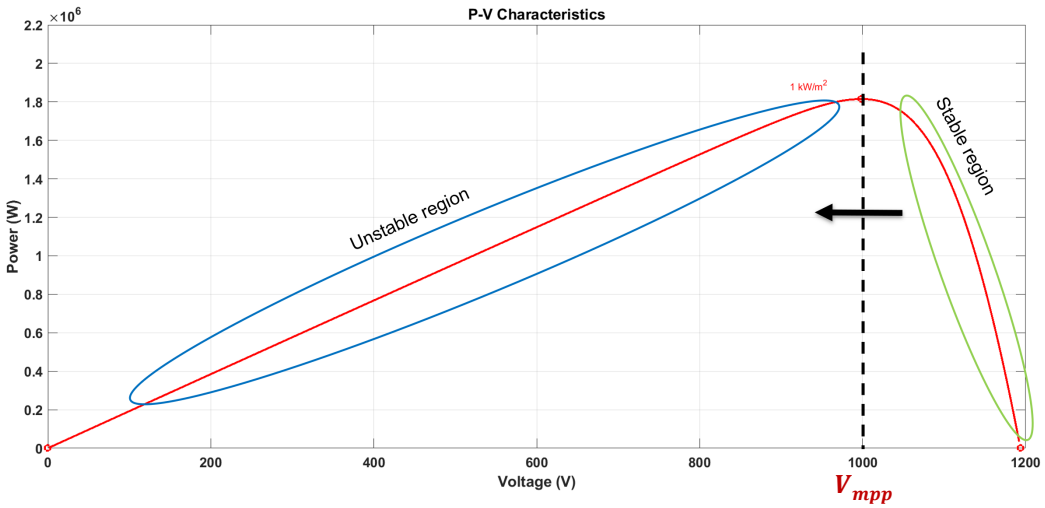


Figure 5. Stable and unstable dc bus voltage regions with a particular irradiance and temperature

Details of the dc voltage control are shown in Figure 6[5]. Once the dc bus voltage (V_{pv}) drops and goes below V_{mpp}, the proportional, integral, and derivative (PID) control will react to generate a negative frequency deviation ($\Delta\omega$). This $\Delta\omega$ will be added to the frequency reference (illustrated in Figure 4) and the frequency generated by the GFM PV inverter will decrease. When there are other generation resources inside the microgrid which have P-f droop and headroom available, they will sense the frequency decrease and increase their generation to balance the load. When there are no other generation resources with P-f droop or when headroom is not available, the frequency will decrease and eventually cause load shedding. In either case, the active power output of the GFM PV inverter will decrease and its dc bus voltage can go back to V_{mpp}. Note that $\Delta\omega$ has an upper limit of zero, which is designed such that the dc voltage control does not have any impact unless the dc bus voltage goes into the unstable region.

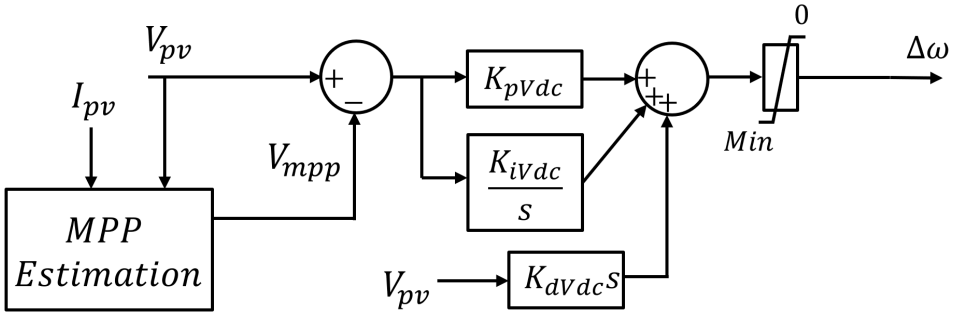


Figure 6. Detailed implementation of dc voltage control

Since V_{mpp} varies with PV irradiance and temperature, a MPP estimation algorithm is required such that V_{mpp} can be updated continuously. This will be discussed in detail in the next section. With dc voltage control, the steady state P-f droop curve of the GFM PV is illustrated by the blue curve in Figure 7. The active power of the GFM PV can vary between zero and the power at MPP (P_{mpp}). Once P_{mpp} is reached and load increases, the GFM PV will reduce its frequency and the final steady state frequency depends on the P-f droop curves of the other generation resources inside the microgrid. For example, assuming there is a diesel generator besides the GFM PV, whose P-f droop curve is shown by the green curve in Figure 7. Consider an initial operating condition where the total load inside the microgrid equals $P_{pv0} + P_{SG0}$. According the to droop curves, the initial frequency is at nominal (f_{nom}). When the load increases, both the GFM PV and the diesel generator increase their generation according to the droop curves. Once the GFM PV output reaches P_{mpp}, the dc voltage control limits its output power at P_{mpp} and the additional load increase is picked up by the diesel generator itself. When the load increases to $P_{mpp} + P_{SG1}$, the system frequency settles at f_{new} which is determined by the two droop curves together.

[5] Z. Chen, R. H. Lasseter and T. M. Jahns, "Power Reserve for Grid-Forming PV Sources with Stability Enhancement in Mixed-Source Microgrids," 2019 IEEE Power & Energy Society General Meeting (PESGM), 2019, pp. 1-5.

In certain scenarios, it is beneficial that the GFM PV does not generate at P_{mpp} but reserve certain active power headroom. This can be done by limiting the dc voltage at a value higher than V_{mpp}. The use case of GFM PV active power reserve will be discussed in the next chapter.

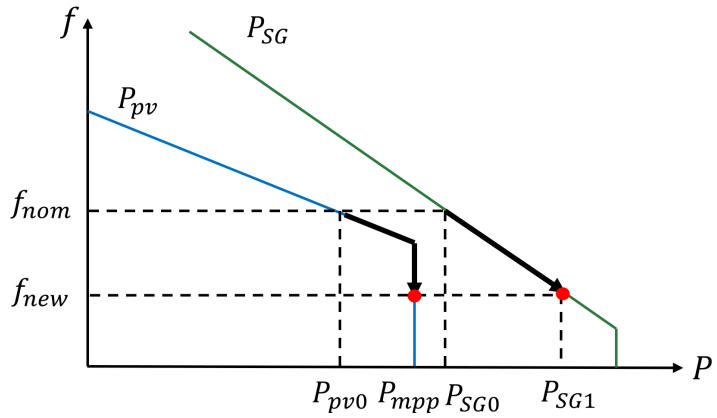


Figure 7. Example P-f droop curves on a GFM PV inverter and a diesel generator to show power sharing

Maximum Power Point Estimation

As discussed, estimating MPP is important for implementing dc voltage control and active power reserve for GFM PVs. It is important to notice that the MPP tracking (MPPT) methods commonly implemented on grid-following PV inverters today can only track MPP when it is operating at or close to the MPP. Since a GFM PV naturally follows the load and can operate with much lower power output than the MPP during low load period, a MPP estimation method is required which is very different from the MPPT methods.

While there are different methods to estimate MPP, a model-based method[6] without the need for irradiance and temperature sensors is considered in this work. The method represents the PV panels by the well-known single-diode equivalent circuit[7] shown in Figure 8. In the equivalent circuit, R_s and R_{sh} are series and shunt resistances, I_{ph} is the current from the PV source, and V_{panel} and I_{panel} are voltage and current measured at the PV panel. Baseline R_s, R_{sh}, and I_{ph} can be directed calculated based on operating points at standard test conditions that are provided in the datasheet.

To estimate the MPP, a few sets of V_{panel} and I_{panel} measurements are first obtained. The equivalent circuit is then used as virtual temperature and irradiance sensor to estimate the irradiance and temperature. Next, the short-circuit current I_{sc} of the PV panel could be

[6] Z. Chen, R. H. Lasseter and T. M. Jahns, "Active Power Reserve Control for Grid-Forming PV Sources in Microgrids using Model-based Maximum Power Point Estimation," 2019 IEEE Energy Conversion Congress and Exposition (ECCE), Baltimore, MD, USA, 2019, pp. 41-48.

[7] S. Kolesnik *et al*., "Solar Irradiation Independent Expression for Photovoltaic Generator Maximum Power Line," in *IEEE Journal of Photovoltaics*, vol. 7, no. 5, pp. 1416-1420, Sept. 2017.

calculated using the current and voltage measurements. Lastly, the MPP current I_{mpp} could be estimated from I_{sc} since I_{mpp} and I_{sc} have a proportional relationship. Once I_{mpp} is identified, MPP voltage V_{mpp} and the MPP could also be estimated using the nonlinear Lambert-W function[6,7].

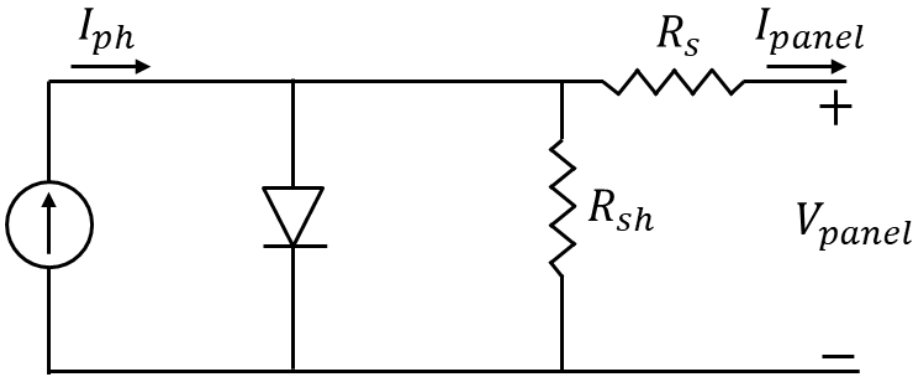


Figure 8. Single-diode equivalent circuit of PV panels

The model-based MPP estimation method is implemented and tested using MATLAB/Simulink. The performance of the model-based MPP estimation is demonstrated in Figure 9, which shows the comparison of actual MPP and estimated MPP with varying irradiance. The orange line illustrates the measured MPPs, and the blue line shows the estimated MPPs. It can be seen that they match well for all the irradiance conditions considered.

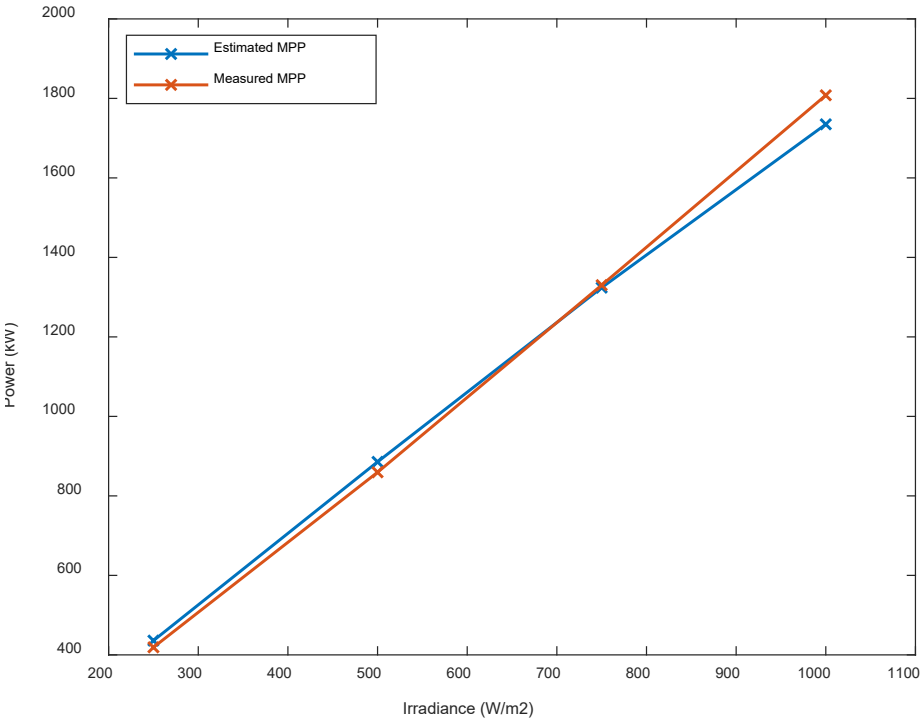


Figure 9. Verification of the implemented MPP estimation method

3 USE CASES OF GRID-FORMING PV PLANTS IN MICROGRIDS

In a microgrid with PV and other generation resources (e.g., BESS, diesel generator), the generation resources all together should provide sufficient active power reserve (APR), both up- and down-reserve, to balance the load. In microgrids with different generation mixes, the need for active power up-reserve (headroom) from GFM PV is different. In this chapter, the concept of APR from GFM PV and the methods to implement it are illustrated. Subsequently, the use cases of APR from GFM PV in microgrids with different generation mixes are discussed. Besides APR, several use cases of GFM PV that also apply to other types of GFM resources are summarized in the last section of the chapter.

Active Power Reserve from GFM PV Plants

In a microgrid with multiple GFM DERs, instead of having one GFM DER support the entire load, the microgrid load should be properly shared across the GFM DERs. In order for GFM DERs to follow the load and to have proper active power sharing in microgrid operation, active power-frequency (P-f) droop as illustrated in Figure 7 can be enabled as the primary control function at each GFM DER. By activating P-f droop control, a GFM DER has the capability to provide down-reserve (i.e., following a load reduction event, as system frequency increases, the down-reserve function enabled in the DER reduces its active power output).

However, P-f droop control does not guarantee up-reserve from a GFM PV plant. When it operates at the maximum power point (P_{mpp} in Figure 7) and load increases, the GFM PV plant cannot further increase its active power output, and its frequency drops as indicated by the vertical power limit line at P_{mpp}. The frequency drop will cause other DERs with remaining reserves to increase the power output and balance the load.

For a GFM PV plant to provide up-reserve, a change in control philosophy is needed to ensure it operates below the P_{mpp} considering irradiance variations. There are different control methods to realize up-reserve in GFM PV plants. Two methods[5] are illustrated and discussed here. With reference to Figure 10, the first method designs the P-f droop curve of the GFM PV plant in such a way that it operates below the MPP. As a result, following a load increase in the system, the GFM PV plant has up-reserve and can increase its active power output to balance the load. However, it should be noted that the steady state output of the GFM PV plant increases following the load increase. The benefit of it is that the PV GFM DER leverages its APR to balance load in steady state, such that other generation resources (e.g., diesel generator) do not need to pick up the entire load increase, therefore reduce the fuel cost. The downside is that the PV APR is reduced at the new steady state. Moreover, the amount of APR changes when P_{mpp} changes with solar irradiance. To ensure sufficient APR, solar irradiance forecast is needed, and the P-f droop settings should be updated periodically (e.g., every 15 minutes) based on the forecast.

In contrast, instead of shifting the P-f droop curve, method 2 constantly shifts the maximum allowed PV output to be less than the maximum available power, thus providing up-reserve. This method ensures that a constant amount of APR is available at steady state with the compromise that the APR is only leveraged during the dynamic period. It does not require solar forecast as the APR is not affected by the change in P_{mpp}.

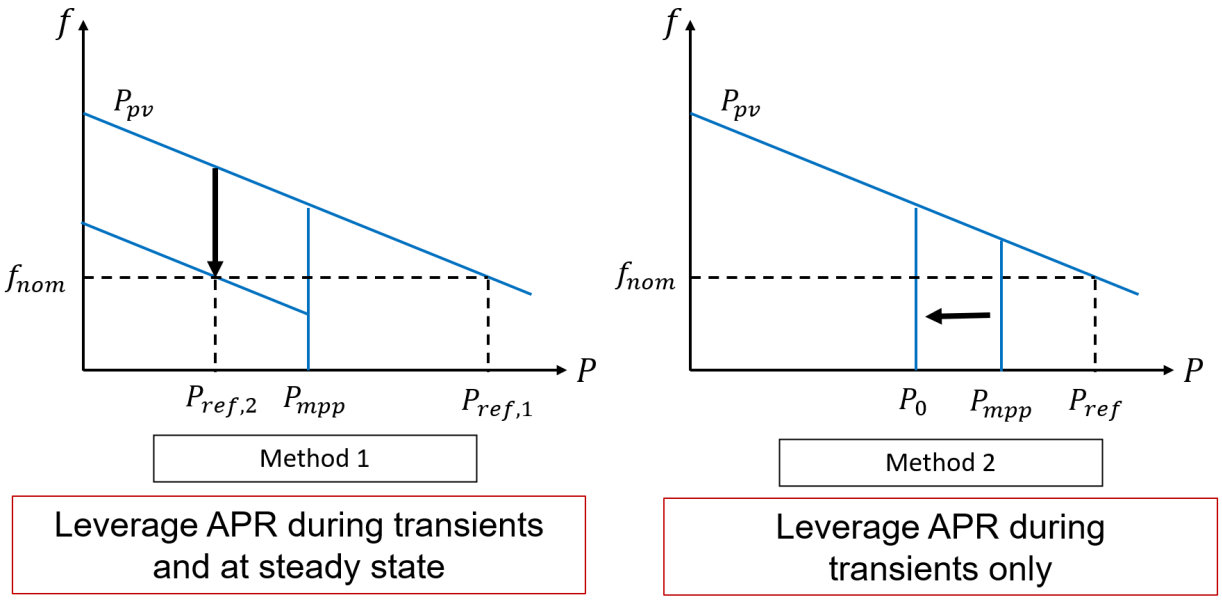


Figure 10. Two control methods to realize up-reserve in GFM PV plants

Figure 27. Figure 11 shows the GFM PV plant response with method 1 and 2 in an example microgrid with a GFM PV plant and a synchronous diesel generator (SG) following a load step increase event. As can be seen, with method 1, the PV output power increases both dynamically and at the steady state after the load increase. On the other hand, method 2 only provide additional power during the dynamic period and the PV output returns to the previous value at steady state. Moreover, the higher active power support from method 1 results in less frequency dip in the microgrid. It is expected that method 1 can work better if the load and PV are well forecasted and the set points for the P-f droop control are dispatched properly and updated periodically by the microgrid controller. Since these assumptions are generally satisfied in the DOE SECURE project, method 1 is selected as the method to implement APR and will be further discussed in the remaining chapters. In contract, method 2 can outperform if the load and/or PV uncertainty is high or not well forecasted.

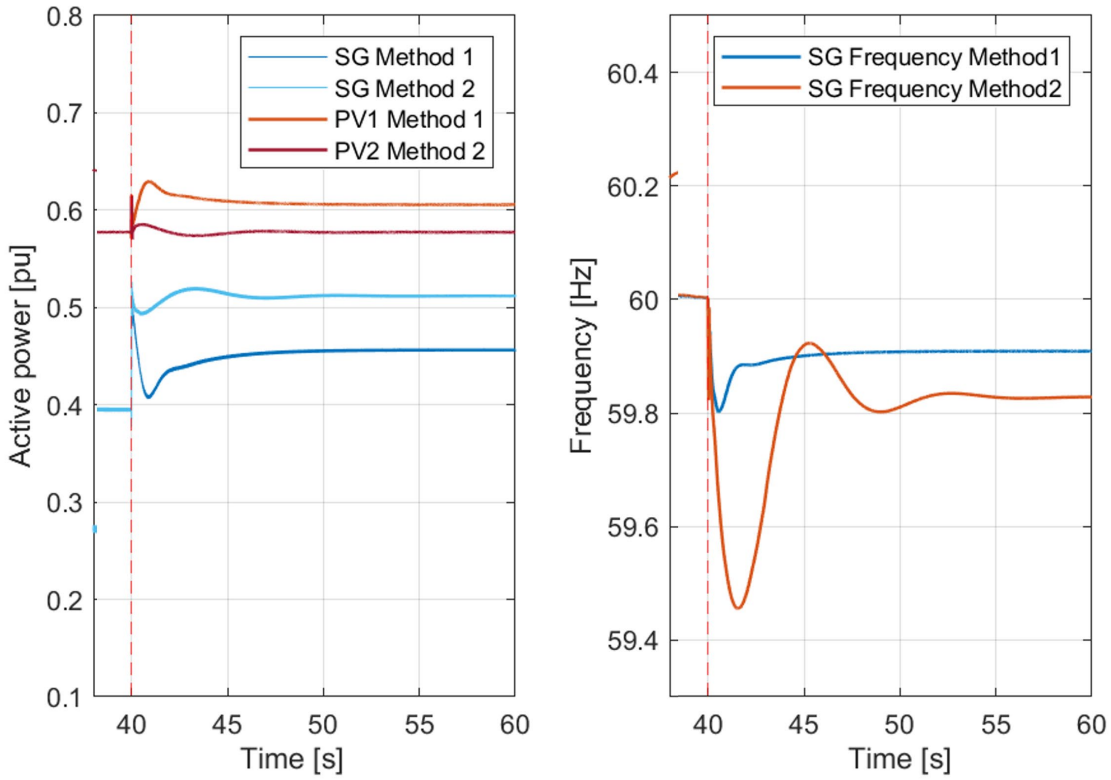


Figure 11. Response comparison between the two APR methods

The P-f droop control and the control technique to maintain APR is local, fast, autonomous, and does not require communication with the microgrid controller in real time (note periodically update of the P-f droop settings, e.g., every 15 minutes, is required with method 1). It is implemented in the primary control layer as illustrated in Figure 12. However, for the GFM DERs to follow the load while maintaining system frequency at the nominal during steady state operation, the slower secondary control layer is needed. Additionally, an even slower tertiary control layer is needed to perform economic dispatch and manage the power reserve for DER considering the load and PV forecast in the microgrid. The secondary and tertiary control layers can be implemented in the microgrid controller to update the dispatch settings to GFM DERs.

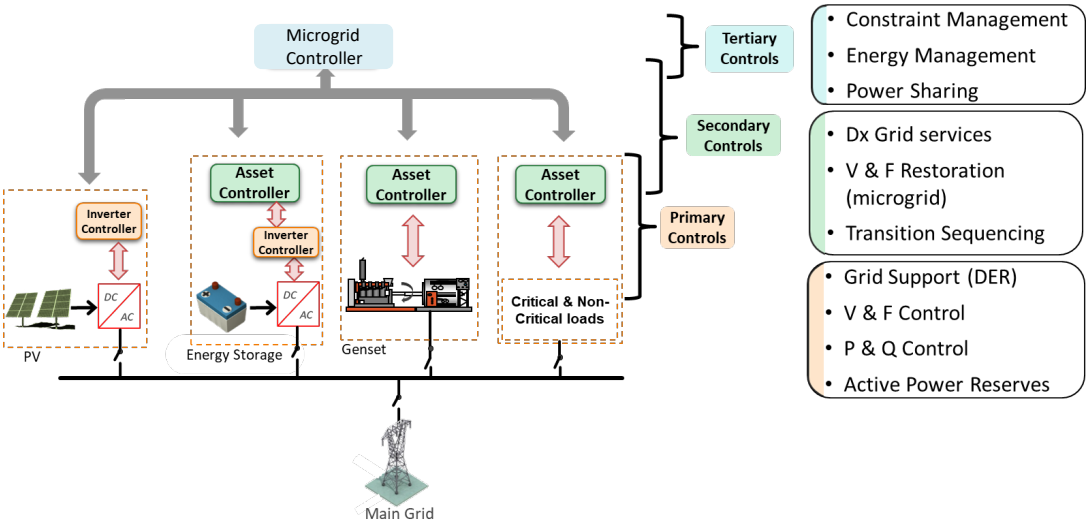


Figure 12. Hierarchical control of DER in a microgrid including APR for GFM PV

Use Case of GFM PV Active Power Reserve in Fully Inverter-Based Microgrids

Following the previous description of the APR concept, this section describes the use case of GFM PV APR in a fully inverter-based microgrid (i.e., without any slower-response resources like diesel generators).

In a fully inverter-based microgrid with high PV penetration, BESS could still be required to supply load during nighttime and during hours when the solar irradiance is low and the loading levels are high. The power and energy rating of the BESS should be designed considering the amount of (critical) load inside the microgrid and the expected operational duration of the microgrid.

In an islanded microgrid, depending on the maximum available PV generation and the loading level, there can be different operation scenarios, which are illustrated in Figure 13. In scenarios (a) and (b), the load is greater than the maximum available PV generation (i.e., excess load). Therefore, the BESS should discharge to balance the load. In scenario (a) where the excess load is greater than the BESS' maximum discharge rate, load curtailment is required to maintain power balance. On the other hand, the available PV generation is higher than load (i.e., excess PV) in scenarios (c) and (d), which can be used to charge the battery. However, when the excess power is greater than the BESS' maximum charge rate, curtailment of PV generation is necessary.

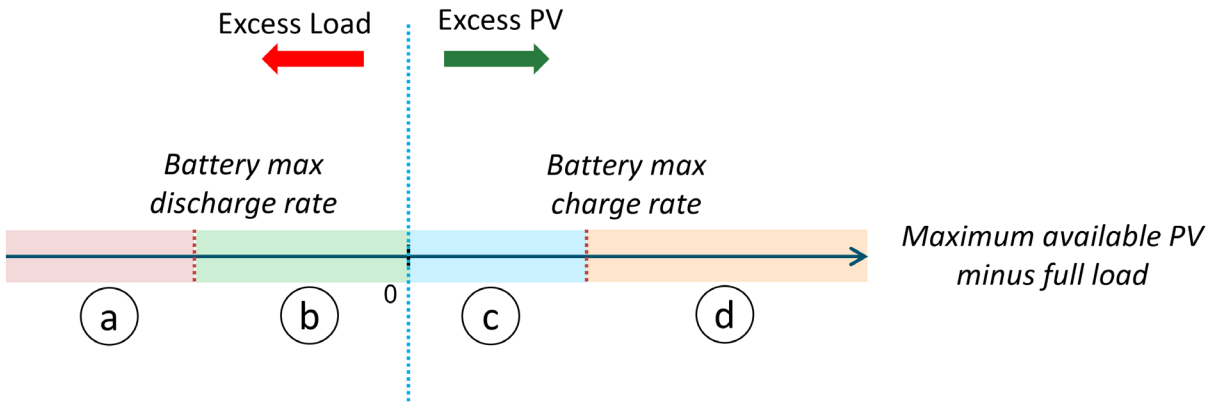


Figure 13. Operation Scenarios in a fully GFM inverter-based microgrid with PV and BESS with PV net load along the horizontal axis. Scenarios: a) load must be curtailed, b) BESS must discharge, c) BESS can charge, and d) PV must be curtailed.

The operation modes of PV, BESS and load corresponding to each scenario are designed as shown in Table 1. Note that when there is excess load, the PV plant is designed to work at MPP to reduce the BESS discharging and thereby increase the duration of microgrid operation. When there is excess PV generation, the PV continues to work at MPP to maximize BESS charging and is only curtailed when the excess PV generation surpasses the BESS' maximum charge rate. With such a design logic, the GFM PV provides down-reserve in all the scenarios. However, it only provides up-reserve in scenario (d) when it is curtailed. In the other scenarios, up-reserve is provided by GFM BESS only. Since both GFM PV and GFM BESS can stabilize microgrid frequency by fast active power support, the up-reserve from BESS is leveraged first and the PV is operating at MPP whenever possible to fully utilize PV generation to increase the possible duration of microgrid operation.

Table 1. Operation modes of PV, BESS and load corresponding to different scenarios

Scenarios		***Operation Mode***		
		PV	***BESS***	***Load***
Excess load	a	MPP	Max discharging	Curtailed
	b	MPP	Discharging	Fully served
Excess PV	c	MPP	Charging	Fully served
	d	Curtailed	Max charging	Fully served

The primary P-f droop control of PV and BESS plants together with the dispatch from the microgrid controller should be properly designed to realize the operation modes. An important factor to consider here is that the maximum charge and discharge rates of BESS are not fixed but vary with the state of charge (SoC) of the battery. P-f settings and the GFM PV requirements to realize these use cases will be discussed in the next chapter.

Use Case of GFM PV Active Power Reserve in Microgrids with Slower-Response Resources

This section presents the use case associated with APR of GFM PV plants in a mixed-source microgrid (i.e., with slower-response resources such as diesel synchronous generators). In this scenario, the APR can be provided by the synchronous generators or the GFM PV plants, or both. However, the slower governor response can cause issues if the APR is solely provided by synchronous generator, which necessitates up-reserves from GFM PV plants.

Compared with fast-responding inverters, the governor response of a synchronous generator is slow. As a result, it picks up the load after a load increase in a much slower rate. In a microgrid with high PV penetration, the inertia level of the system is low. This coupled with the slower governor response of synchronous generators can result in large frequency drop following a load increase.

This phenomenon is demonstrated with simulation studies. An example microgrid based on modified IEEE 13 bus feeder with 2 GFM PV plants and a synchronous generator is considered as shown in Figure 14. When the active power reserve is provided by the synchronous generator only and the GFM PV plant is working at its maximum power point, after a 400 kW (around 10% of the total microgrid load) load increase, the dynamic response of the GFM PV plant and synchronous generator is shown in Figure 15 (case 1). As can be seen, the frequency dips to 58 Hz which may cause under-frequency load shedding in the system. If the amount of load increase is higher, the frequency dip could be more severe which may cause tripping of the grid-following DERs (e.g., behind-the-meter PV) in the microgrid according to IEEE Std 1547™-2018. The large frequency dip is mainly caused by the slower active power response from the synchronous generator.

As comparison, besides the synchronous generator, the PV GFM DER is providing active power reserve and pick up half of the load increase in a second study. The system response after the 10% load increase is shown in Figure 15 (case 2). In this case the lowest system frequency during the dynamic period is 58.75 Hz, which is much higher than the previous case. Moreover, the frequency dynamics settles down much faster in this case. Due to the fast response rate of the GFM PV plant, with active power reserve, it can improve system frequency stability and avoid unnecessary under-frequency load shedding and/or tripping of grid-following DERs in a mixed-source microgrid with slower-response resources.

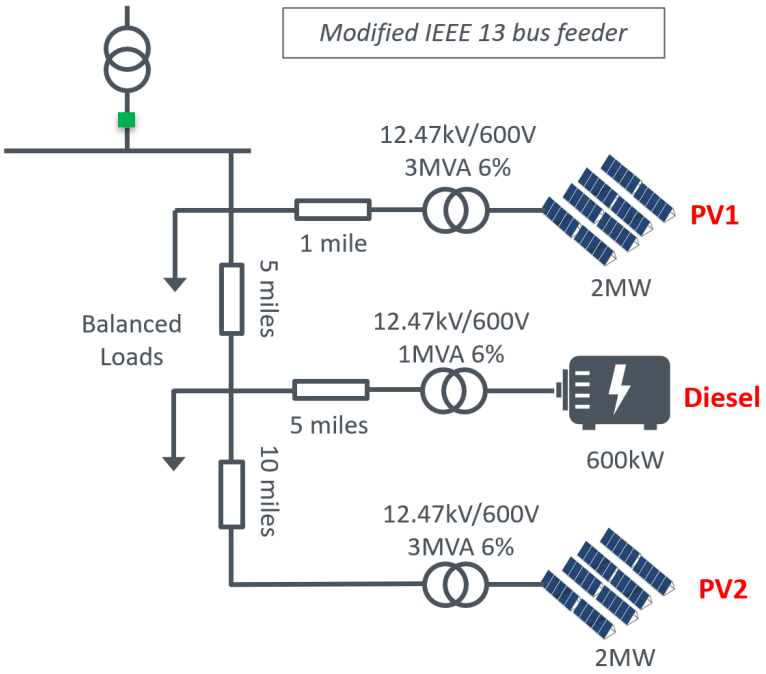


Figure 14. Example mixed-source microgrid based on modified IEEE 13 bus feeder

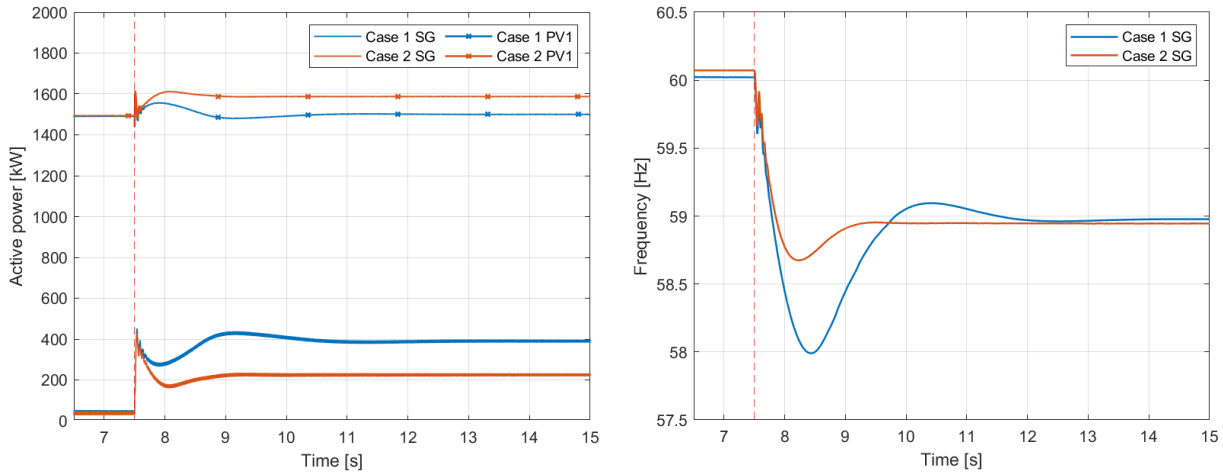


Figure 15. Comparison of active power and frequency responses without PV APR (case 1) vs with PV APR (case 2)

General Use Cases

Besides APR, GFM PV plants can provide other use cases in microgrid applications such as regulating microgrid voltage and improving microgrid stability. Such use cases are not unique to GFM PV but apply to other types of GFM resources (e.g., BESS, diesel generator) as well. Here several use cases are illustrated with high level discussion on the performance requirements to fulfil the use cases. More details are covered in a previous tech update[3].

Use case to support unbalanced load and maintain voltage balance

Description of the use case

Since unbalanced load typically exists in a community microgrid, it is important that a GFM DER can supply the unbalanced load while maintaining the voltage unbalance on the three-phase feeder inside a microgrid within a certain limit. If the voltage unbalance is severe, it can lead to motor derating and potentially cause damage to three-phase induction motor loads inside the microgrid.

GFM DER performance requirements to fulfil the use case

If the microgrid is effectively grounded, the voltage unbalance caused by unbalanced load will appear in the form of negative sequence voltage. Therefore, it is important that the GFM DER has negative sequence voltage control and regulate the negative sequence voltage inside the microgrid. A performance requirement for GFM DER can be developed as:

"A grid-forming power plant should maintain balanced voltage at its reference point of applicability (RPA) when it operates within the negative sequence current capability and total current capability. The negative sequence current capability should be greater than x pu". Notice the value of x depends on specific microgrid loading conditions and should be set forward based on detailed studies of a particular microgrid.

To adapt this requirement to the scenario with multiple GFM DERs, each GFM DER should contribute certain amount of negative sequence current to reduce unbalanced voltage in the microgrid. Whether each GFM DER should still regulates its RPA voltage to be balanced or share the negative sequence current contribution through certain droop control logic needs further investigation.

Use case to support nonlinear load and restrict voltage harmonics

Description of the use case

When there is nonlinear load inside a microgrid, voltage harmonics become a concern if the generation sources fail to provide sufficient harmonic current to the nonlinear load. Voltage harmonics can cause a number of issues. There can be increased heating stress due to the copper and/or iron losses at the harmonic frequencies, which may lead to faster deterioration of equipment. Specifically, for motor loads, the harmonic voltage may induce torque pulsations. Certain harmonic frequency components may generate counter electromotive forces, which affect the rotational speed of the motor. Therefore, it is important that the GFM DER can supply the nonlinear load while maintaining sufficiently low voltage harmonic distortion inside the microgrid.

GFM DER performance requirements to fulfil the use case

Since a GFM needs to provide higher amount of harmonic current in order to limit the harmonic voltage in the system, a related performance requirement for a GFM DER can be developed as:

"A grid-forming power plant should maintain voltage THD at its RPA to be below x% when operating within its physical limits. And it should have a crest factor higher than y". Having a crest factor larger than one means the GFM DER can inject harmonic current to the system to supply the nonlinear load. Note the values of x and y depend on particular microgrid design and should be determined based on detailed study of a particular microgrid.

With multiple GFM DERs, each GFM DER should contribute certain amount of harmonic current to reduce the voltage harmonics in the microgrid. How to design the requirements such that the voltage harmonics can be properly controlled, and the harmonic current is shared properly between the GFM DERs needs further investigation.

Use case to black start the microgrid

Description of the use case

For microgrid operation, it is important that at least one GFM DER inside the microgrid can black start the microgrid following a predefined cranking path. When black starting a microgrid, the GFM DER should be able to provide the in-rush current and power needed by transformer and induction motor start-up, while maintaining acceptable voltage and frequency in the system. While in theory a GFM PV plant should be able to black start the microgrid when there is sufficient irradiance and available power, lab testing is underway to demonstrate this capability. It should be noted that black start using a GFM PV plant is not as reliable as a GFM BESS since the PV available power is intermittent. Therefore, in a microgrid design with other GFM resources (e.g., BESS or diesel generator) besides PV, the other GFM resources can be leveraged to crank start the microgrid while GFM PV can be connected once the feeder (or a section of the feeder) is energized.

GFM DER performance requirements to fulfil the use case

Example performance requirements of a GFM DER to black start the microgrid are:

1. The GFM DER should be able to black start itself, including the local auxiliary load and establish an open circuit voltage at the plant RPA without the utility grid. This may indicate an internal power supply for starting the control and communication circuit.

2. The steady state voltage requirements (maintaining acceptable steady state voltage range, regulating negative sequence voltage and voltage harmonics) still apply during temporary steady state period in the black start sequence, except that the steady state voltage range may be relaxed by the operator.

3. If the MV feeder inside the microgrid is four-wire grounded, and the microgrid is not otherwise effectively grounded during the microgrid start-up process, the GFM DER should have a grounding source to reduce voltage unbalance in normal operation and limit the possible temporary overvoltage caused by single line to ground fault.

4. If the GFM inverter and the dc source are not sufficiently oversized to provide the inrush current and motor start up power while staying within the continuous rating, short-term current and power capability should be required. The amount of short-term current and power rating required depends on the load characteristics and the black start sequence.

4 REQUIREMENTS AND SPECIFICATIONS FOR GFM PV PLANTS ACTIVE POWER RESERVE FUNCTION

This chapter presents the performance requirements and specifications developed for APR from GFM PV plants inside a community microgrid. The specifications are developed for different use case scenarios where the APR function in PV plants is deployed alongside inverter-based (i.e., BESS) and non-inverter based (i.e., synchronous generators) DER in a microgrid.

As discussed in chapter 3, GFM PV plant with up-reserve can be used to improve frequency dynamics when there are slower-response resources such as synchronous generators. Down-reserve of the GFM PV plant should be utilized with or without slower-response resources to handle load uncertainty.

In this chapter, the APR specifications developed for the scenario without slower-response resources are illustrated first followed by the specifications with slower-response resources. In both cases, the specifications are designed such that the microgrid steady state frequency is within an acceptable region defined by the microgrid operator and the frequency dynamics do not trigger tripping of the grid-following DERs or unnecessary load shedding when the planned worst-case load change event is considered. Note the specifications are developed considering APR method 1 described in chapter 3 (see Figure 10).

Requirements and Specifications in Fully Inverter-Based Microgrids

The primary P-f droop control of PV and BESS plants together with the dispatch from microgrid controller should be properly designed to realize the operation modes. An important factor to consider here is that the maximum charge and discharge rates of BESS are not fixed but vary with the state of charge (SoC) of the battery. If the SoC is low, a BESS can charge at a higher charge rate and make better use of the excess PV generation. When the SoC is close to fully charged, the BESS may limit or reduce the charge rate and when the SoC is full, the BESS cannot charge any more.

As a result, fixed droop settings of the PV and BESS plants cannot achieve the operation modes shown in Table 1. Instead, the microgrid controller should closely monitor the SoC of the BESS and the resulting maximum charge and discharge rates. This requires the BESS to be able to send information regarding its SoC to the microgrid controller. Based on this information and the load and PV forecast, microgrid controller can then dispatch the P-f droop settings of GFM PV and BESS plants through tertiary control. Since the droop settings will be updated periodically, both the GFM PV and BESS should have the capability to modify their droop settings (both reference values and the droop slope) through commands issued by the microgrid controller.

Steady state requirements

To maintain appropriate steady state frequency in the microgrid, the P-f droop settings of the GFM PV plant and the BESS needs to be adjustable by the microgrid controller. Based on the current conditions of the DER (i.e., BESS SoC and PV irradiance), a few methods to determine the droop curves of PV and BESS are proposed and described next. Note that for all the scenarios, it is assumed that the forecasts on PV available power and load are available to the microgrid controller when selecting and applying the settings during island operations. Moreover, the settings are general in the sense that it applies to all the scenarios shown in Figure 13, regardless of whether the PV available power is higher or lower than the load.

Scenario 1: SoC of the BESS is low, minimize battery discharging and maximize battery charging

When the SoC of the BESS is low, the P-f droop curve settings in Figure 16 are enabled in the PV and BESS plants to maintain steady state frequency within an acceptable range whenever possible. In this scenario, the microgrid controller will operate to minimize battery discharging and maximize charging by enabling such settings in the GFM PV and BESS. Therefore, if the available PV (Ppv_mpp) is less than the load, PV operates at MPP reducing the discharge rate of BESS. If the excess load is higher than the BESS' maximum discharge rate, it indicates that the total available generation in the microgrid is less than the load. This will drive the BESS frequency to drop along the vertical line section (Pb_maxd) and eventually trigger the underfrequency loading shedding. Note that the BESS discharge rate is restricted in this scenario because the SoC is low.

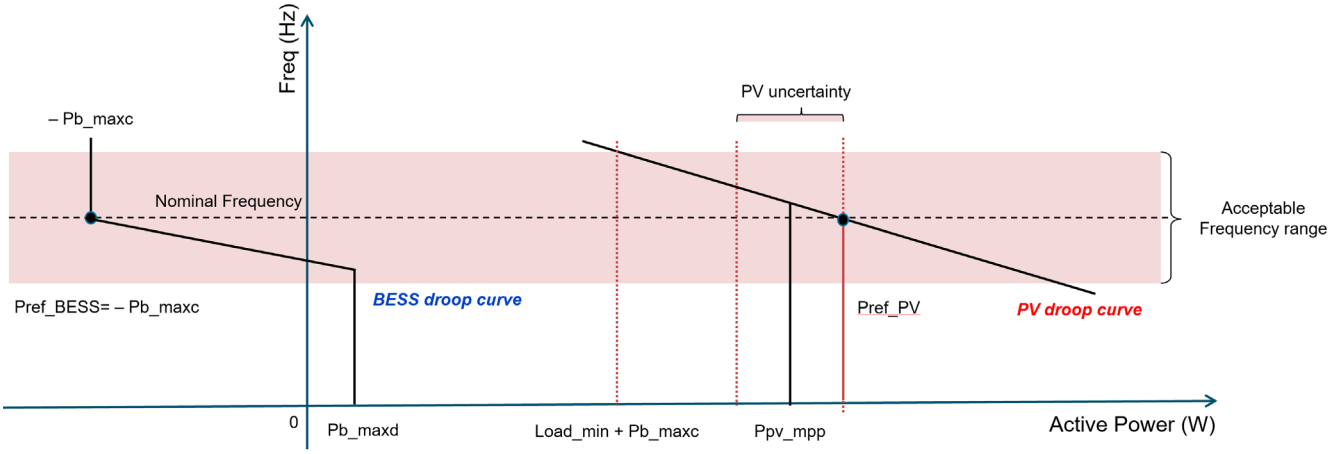


Figure 16. P-f droop settings for PV and BESS plants when SoC of the BESS is low

When the available PV is greater than the load, PV continues to operate at MPP. Suppose if the excess PV power (PV output minus load) exceeds the BESS' maximum charge rate (Pb_maxc), the battery no longer follows the slope section of the droop curve in Figure 16. It starts tracking the vertical line section (-Pb_max) in the BESS droop curve, that increases the frequency output. This rise in output frequency further reduces/curtails the PV output power along its droop curve.

Scenario 2: SoC of the BESS is high, minimize battery discharging and limit battery charging

When the SoC of the battery is high, the microgrid controller chooses the droop settings in Figure 17 and updates the PV and BESS. As a result, the battery limits its charge rate to be significantly less than the maximum charge rate. These settings minimize battery discharging when there is excess load and charges the battery (at a limited rate) when there is excess PV generation. With the settings in Figure 17, if the available PV is less than the load, PV works at MPP and therefore the BESS discharge rate is minimized. When the available PV is greater than the load, PV keeps working at MPP and the excess PV power is used to charge the battery. If the excess PV power exceeds the BESS' charge rate limit as indicated by the vertical line section in BESS' droop curve (Pref_BESS), the battery no longer follows the slope section of the droop curve in Figure 17. It starts tracking the vertical line section (Pref_BESS) in the droop curve that increases the frequency, and the PV output power gets curtailed. Note this charge rate limit (Pref_BESS) is significantly less than the maximum charge rate (-Pb_max) to protect the battery since the SoC is high.

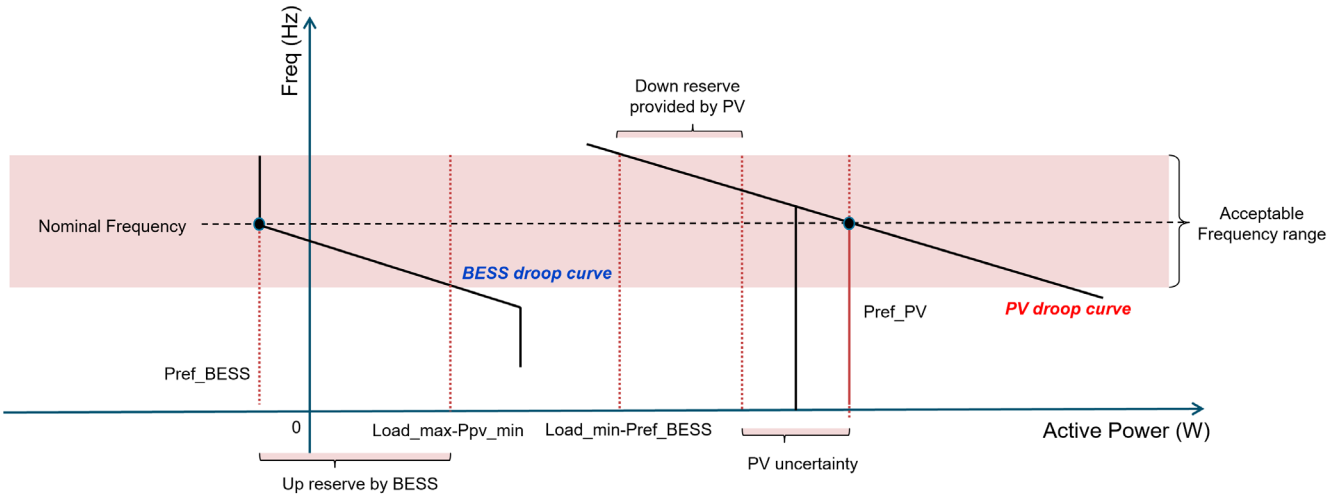


Figure 17. P-f droop settings for PV and BESS plants when SoC of the BESS is high

Scenario 3: SoC of the BESS is 100%, minimize battery discharging and no battery charging

When the SoC of the battery is 100%, the microgrid controller chooses the droop settings in Figure 18 and updates the PV and BESS such that the battery cannot charge any more. With these settings, if the available PV is less than the load, PV works at MPP and therefore the discharge rate of BESS is reduced. When the available PV is greater than the load, system frequency increases and the PV output power gets curtailed similar to the previous scenarios.

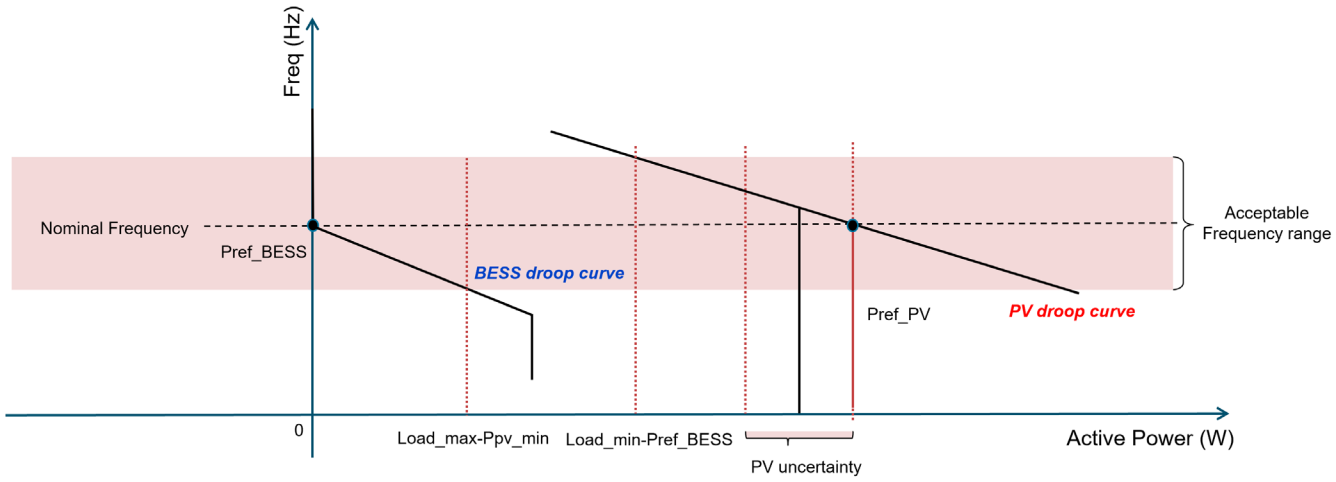


Figure 18. P-f droop settings for PV and BESS plants when SoC of the BESS is 100%

In summary, for all the three scenarios, the droop curve for PV can be set as a straight line between the points (Load_min-Pref_BESS, Freq_high) and (Ppv_max, Freq_norm). Note that the points are illustrated as active power-frequency pairs, and Freq_high and Freq_nom denote the upper bound of the acceptable frequency range and the nominal frequency, respectively. For BESS, the droop curve can be set as a straight line between the points (Load_max-Ppv_min, Freq_low) and (Pref_BESS, Freq_norm), where Freq_low denotes the lower bound of the acceptable frequency range.

Dynamic/transient requirements

In all the scenarios discussed above, whenever the PV available power is less than the load, the PV works at MPP such that the discharge rate of BESS is reduced, which increases the duration of the islanded microgrid, enhancing resiliency. Moreover, with this design, the up-reserve in the island is primarily provided by BESS while the PV primarily provides down-reserve, thereby, minimizing the discharge rate of BESS and maximizing its charging whenever possible. This can be done because both BESS and PV plants are inverter-based and they both have the capability to respond fast to adjust the active power output following a change in load.

However, even though inverter-based plants are able to respond fast, without explicit requirements, the dynamic response of the plants may not be sufficient to maintain stability and acceptable frequency dynamics following a load disturbance. Therefore, in this section, dynamic/transient requirements for the GFM plant are developed to ensure stable and acceptable frequency dynamics in the microgrid. A microgrid with multiple inverter-based GFM plants is considered and the requirements for each individual plant are presented first. Subsequently, a setting guideline is presented to limit the overall frequency deviation and maintain microgrid stability considering the interaction between multiple GFM plants.

Requirements on a single GFM plant

The dynamic frequency requirements developed in this subsection are to be applied under system "normal operating conditions", where the active and reactive power as well as current output from the GFM plant are expected to be within its continuous or short-term rating following the disturbance. Note that in standards addressing grid-connected DERs such as IEEE Std 1547™-2018, normal operating conditions are defined by grid voltage and frequency within a certain region. However, in microgrid operations, since the voltage and frequency of the microgrid is largely governed by the GFM plants, it is proposed here to define the "normal operating condition" based on system events. For example, if the microgrid is designed and the GFM plant sized to handle load step change up to 20% of the microgrid peak load without causing damage to sensitive load or tripping of the grid following DERs, then load step changes under 20% are included in normal operating conditions.

In contrast, more severe disturbances such as a low impedance fault in the microgrid can lead to abnormal operating conditions under which the GFM plant is likely to reach its physical limits (e.g., current limit) and a different set of requirements are applicable.

The proposed requirements are constructed as follows (more details are discussed in a previous tech update[3]):

- Considering a scenario where a composite load is connected at the reference point of applicability (RPA) of the GFM plant, and the kVA rating of the load is x_1% of the GFM plant rating (x_1 should be specified between 0 and 100). x_2% of the load is three-phase induction motor load while the rest is constant impedance load with a power factor of x_3

- Following specified load change events (e.g., motor start up, load rejection), the GFM plant should maintain its RPA frequency and voltage to be within specified regions as illustrated in Figure 19 and the maximum rate of change of frequency (ROCOF) should be less than x_4 Hz/s

- If voltage or frequency oscillations occurs following the event, it should have a damping ratio greater than x_5%

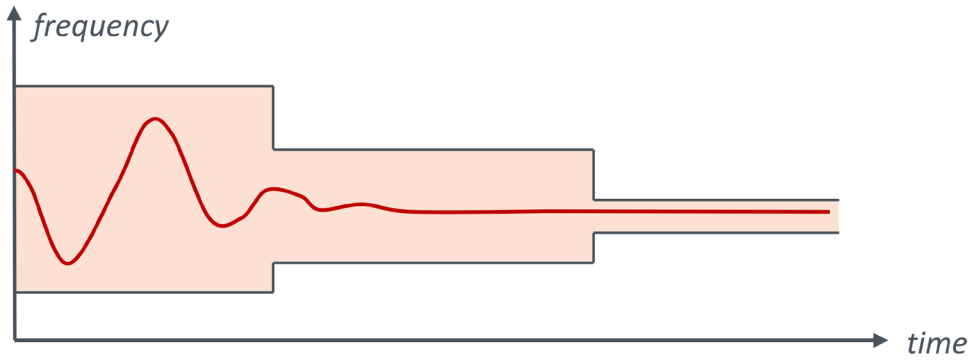


Figure 19. Illustration of the allowed frequency region following the specified disturbances

As the voltage and frequency dynamics inside the microgrid are not only determined by the GFM plant but also affected by dynamic loads and equipment in the system and the interaction between them, ideally, the requirements can be established considering a detailed microgrid model including the dynamic loads and equipment. However, such a detailed model may not be practical. Therefore, the requirements are developed based on a generic composite load model.

With this model, the worst-case load disturbance under normal operating conditions inside the microgrid is then constructed by specifying the rating of the load, the percentage of the motor load and a set of specified load change events. With the load disturbance, the GFM plant is then required to regulate the frequency and the ROCOF at the plant RPA to be within a specified region. Since the frequency dynamics should not cause momentary cessation or tripping of the grid following DERs to avoid cascading effects, the frequency region and the ROCOF should be specified inside the ride through region of the grid following DERs (e.g., inside the ride through region defined in IEEE Std 1547™-2018). Moreover, if oscillation occurs, sufficient damping ratio is required to make sure the system is stable, and the oscillation is damped down fast enough.

Setting guideline considering the interaction between multiple GFM plants

The requirements for individual plant are sufficient when there is only one GFM plant in the microgrid. When there are multiple GFM plants, the individual plant requirements should still apply to improve the performance of the overall system. However, they are no longer sufficient to guarantee acceptable frequency dynamics and stability considering the interaction between multiple GFM plants. To improve upon the individual plant requirements, this subsection presents a setting guideline to set the droop slopes of the various GFM plants.

GFM control and assumptions

We first consider a microgrid with 100% power electronic sources consisting of a GFM BESS and several GFM PV plants (with *N* inverters total). In this setting, we assume that the voltage phase angle of the inverter with index k is controlled using standard droop control

$$\omega_k - \omega_0 = m_{p,k}(P_k^* - P_k)$$

where ω_k is the frequency of the ac voltage waveform imposed at the inverter bus, ω_0 is the nominal frequency, $m_{p,k}$ is the frequency droop coefficient, P_k^* the inverter active power setpoint, and P_k denotes the inverter's active power injection. The frequency droop coefficient $m_{p,k}$ and reserves of the PV inverter need to be selected to ensure that the maximum frequency deviation $\|\Delta\omega_k\|_\infty = \|\omega_k - \omega_0\|_\infty$ for all inverters k remains within the maximum deviation $\Delta\omega_\infty$ for a given maximum load perturbation ΔP_∞.

Considering the reserve strategy described in the steady state requirements section, this problem reduces to selecting the frequency droop coefficients $m_{p,k}$ which in turn, for every operating point, defines the required reserves.

Average microgrid frequency dynamics

To this end, we first consider the average frequency deviation $\Delta\bar{\omega} = \frac{1}{N}\sum_{k=1}^{N}\omega_k - \omega_0$ that plays a similar role to the center of inertia frequency in a multi-machine system. A straightforward calculation reveals that the maximum average frequency deviation due to a load step of size ΔP_∞ is given by

$$\|\Delta\bar{\omega}\|_\infty = \left(\sum_{k=1}^{N} m_{p,k}^{-1}\right)^{-1} \Delta P_\infty$$

For a microgrid with sufficiently strong coupling (i.e., sufficiently high short circuit ratio at the inverter buses) and frequency droop gains that are sufficiently uniform (up to scaling by the inverter rating), the average frequency is a suitable approximation for the local bus frequencies. However, in a microgrid with weak coupling the local bus deviations from the average frequency may be significant.

Frequency deviations from the average frequency in weakly coupled microgrids

To analyze this aspect, we consider a standard small-signal model that uses the DC power flow approximation $P - P^* = -L\theta - \Delta P$, where P is the vector of power injections and θ (relative to a frame rotating at the nominal frequency) is the vector of bus voltage phase angles, and L is the nodal admittance matrix. Moreover, we require the assumption that $m_{p,k} = \frac{m_p}{\gamma_k}$ for all k. Here m_p is a homogeneous droop coefficient and γ_k is the rating of the inverter with index k. This assumption is often justified by the goal to induce so-called fair power sharing between inverters in steady state. Moreover, it stands to reason that the inverter power limits and reserves scale with the rating, i.e., an inverter with low rating cannot provide the same reserves or frequency droop as an inverter with large rating. By the above assumption, $m_{p,k}$ increases as the converter rating γ_k decreases, i.e., the droop control requires less reserves and power capability to implement.

This results in the model

$$\omega - \bar{\omega} = -m_p\Gamma^{-1}L\theta - m_p\Gamma^{-1}\Delta P$$

Where Γ is a diagonal matrix whose diagonal entries are the inverter ratings γ_k. A standard calculation of the input-output gain of this linear time-invariant system results in the bound

$$\|\omega - \bar{\omega}\|_\infty \leq m_p\gamma_{min}^{-\frac{1}{2}}\left(\frac{\lambda_{max}}{\lambda_2} + 1\right)\Delta P$$

Where γ_{min}denotes the smallest inverter rating and λ_2 and λ_{max} denote the second smallest and largest eigenvalue of the weighted nodal admittance matrix $\Gamma^{-0.5}L\Gamma^{-0.5}$. Even for relatively simple networks, closed form expressions cannot be obtained for λ_2. However, a common

heuristic for radial networks is that λ_2 is approximately the smallest line susceptance, i.e., λ_2 scales with the weakest line in the network. Moreover, λ_{max} is bounded by

$$\lambda_{max} \leq \left(1 + \frac{\gamma_{max}}{\gamma_{min}}\right) \max_k \sum_n \frac{1}{l_{nk}\gamma_k}$$

where l_{nk} denotes the inductance between bus k and n. In other words, the bound on λ_{max} increases if an inverter is connected to many other inverters through connections with low inductance and it increases if the inverter rating is lowered. *Thus, the deviation from the average frequency increases if the microgrid contains inverters with significantly different ratings and if the connectivity is not uniform, i.e., some inverters have weak connections to the remainder of the network while other inverters have strong connections to the remainder of the network.*

Tuning guidelines to limit the overall frequency deviation

Thus, the overall frequency deviation can be bounded as the sum of the deviation of the average frequency and the deviation of bus frequencies from the average

$$\|\Delta\omega\|_\infty \leq \|\Delta\bar{\omega}\|_\infty + \|\omega - \bar{\omega}\|_\infty$$

The preceding analysis shows that specifications on the average frequency deviation for a given maximum load perturbation can be achieved by selecting the frequency droop gains according to $\frac{\Delta P_\infty}{\Delta\bar{\omega}_\infty} = \sum_{k=1}^{N} m_{p,k}^{-1}$.

Moreover, to bound the overall frequency deviation one must consider the deviation $\|\omega - \bar{\omega}\|_\infty$ of the individual bus frequencies from the average. While the analysis of $\|\omega - \bar{\omega}\|_\infty$ depends on quantities that may not be known accurately or are hard to compute in practice, it nonetheless reveals tuning guidelines for microgrids with significantly different ratings and/or significantly different coupling strengths between buses. Specifically, it can be seen that $\|\omega - \bar{\omega}\|_\infty$ can be decreased by further decreasing the inverter droop gains (i.e., making each GFM inverter regulate the frequency more tightly) and that doing so may be required in microgrids with inverters with significantly different ratings and/or significantly different coupling strengths between buses.

Simulation demonstration

To demonstrate proper microgrid operation and stability with the developed performance requirements and specifications, a GFM PV inverter model with APR function has been developed in MATLAB/Simulink. The P-f droop settings of the inverter model can be adjusted according to the specification approach illustrated in Figure 16 through Figure 18. Moreover, the dynamic parameters of the GFM PV inverter control are properly tuned to satisfy the dynamic/transient requirements described above.

An example microgrid with PV and BESS is considered which consists of the IEEE 13 bus feeder with modified generation and loads, as shown in Figure 20. The total capacity from PV is 4 MW which is around 86% of the total generation capacity inside the microgrid.

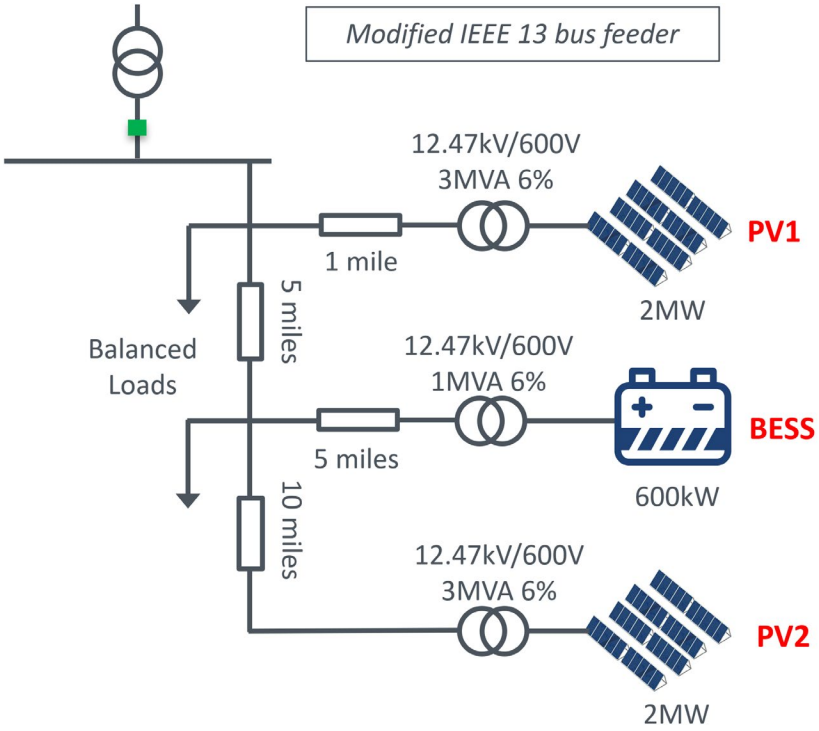


Figure 20. Example fully inverter-based microgrid based on modified IEEE 13 bus feeder

Case study 1: 10% load step increase

A base case is considered where the load in the microgrid is 3000 kW and each PV plant is working at MPP outputting 1800 kW while the BESS is charging at 600 kW. A disturbance is then applied at t=7.5s where the load in the system has a step increase to 3300 kW (10% increase). Based on the droop settings, it is expected that the PV keeps operating at MPP (1800 kW) while the BESS decreases its charging to 300 kW to balance the load. In other words, the up reserve is provided by the BESS alone. Simulation results following the disturbance is shown in Figure 21. As can be seen, the BESS quickly decreases its charging to balance the load while PV continues working at MPP. Since the BESS response is fast, the frequency dip is minimal. Moreover, the dc voltage of the PV inverters is properly controlled with sufficiently low transients. Therefore, it demonstrates that this setting design results in proper dynamic performance besides the steady state benefit (leveraging PV output to the extent possible).

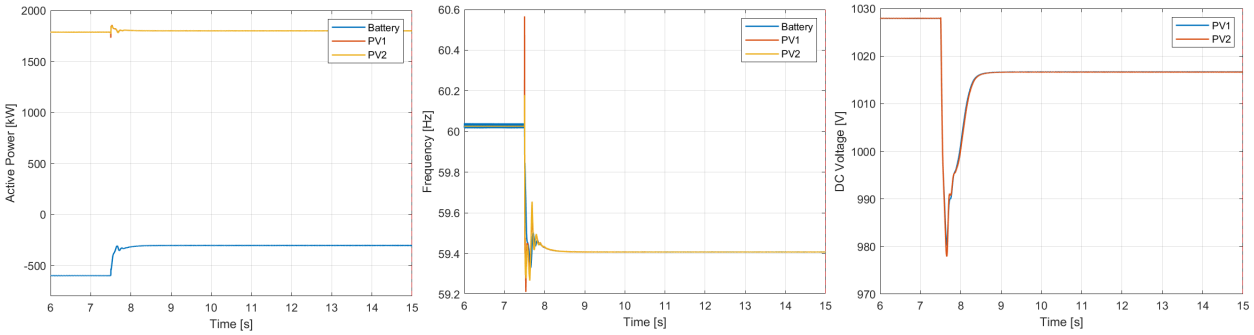


Figure 21. Response from PV and BESS following the load step increase

Case study 2: 10% load step decrease

The performance of the microgrid under a load step decrease event is then considered. Starting again from the base case where the load in the microgrid is 3000 kW and each PV plant is working at MPP outputting 1800 kW, a disturbance is applied at t=7.5s where the load in the system is reduced by 10%. Based on the droop settings, it is expected that the BESS will maintain maximum charging at 600 kW while each PV plant reduces its generation by 150 kW. In other words, the down reserve is provided by the PV plants alone. Simulation results following the disturbance is shown in Figure 22. As can be seen, both PV plants quickly decrease their output to balance the load while the BESS keeps operating at maximum charging. The frequency transient is small and damped down quickly, and the dc voltage of the PV inverters is again properly controlled. Therefore, it demonstrates that the microgrid following the developed setting approach for BESS and PV plants has proper steady state and dynamic performance.

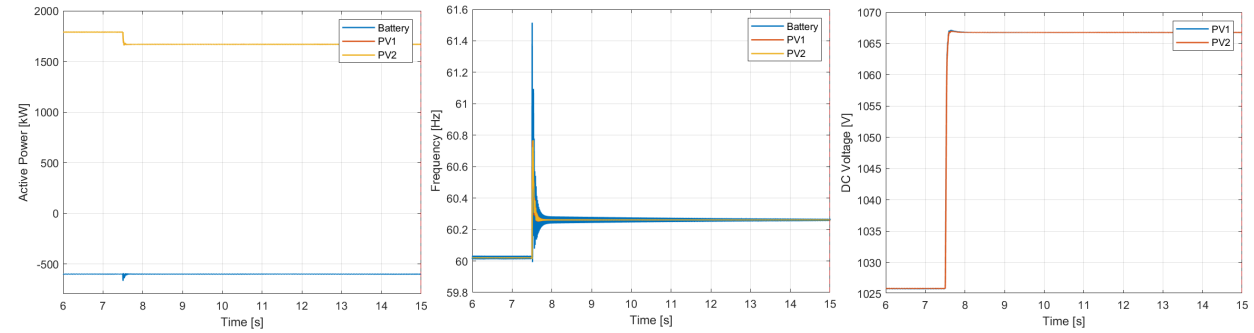


Figure 22. Response from PV and BESS following the load step decrease

Case study 3: 10% irradiance decrease at PV1

For a GFM PV inverter, it should provide APR according to the setting approach at different irradiance level and have proper dynamic performance during irradiance change. To test this aspect, performance of the microgrid under an irradiance change event at one of the two PV GFM plants is considered. Starting from the same base case condition, a disturbance is applied

at t=7.5s where the irradiance at the PV plant PV1 is reduced by 10%, which results in the maximum available power at PV1 to reduce by 10%. Based on the droop settings, it is expected that PV1 will reduce its generation by 180 kW, PV2 will keep its output unchanged, and the BESS will reduce its charging by 180 kW. Simulation results following the disturbance is shown in Figure 23. The steady state results match the droop settings, as the generation from PV1 reduces and so is the charging of the BESS. The transients in power, frequency and dc voltage are all damped down fast without significant oscillations, which again demonstrates that the microgrid following the developed setting approach for BESS and PV plants has proper steady state and dynamic performance.

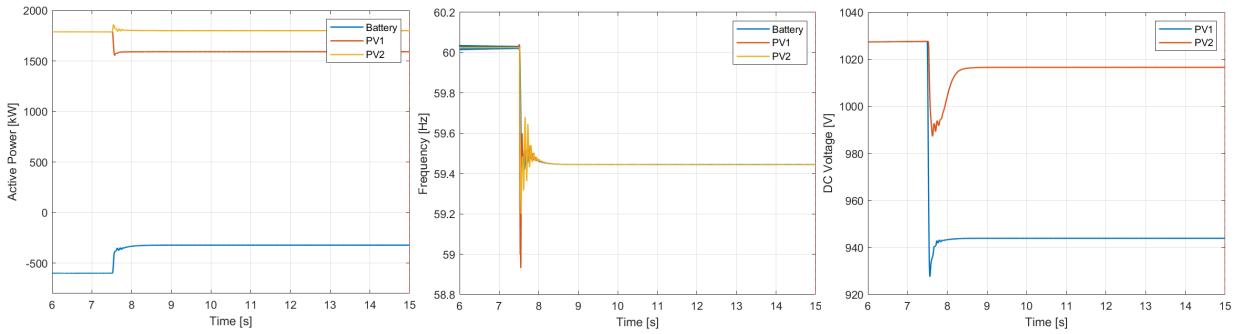


Figure 23. Response from PV and BESS following the irradiance decrease

Requirements and Specifications in Microgrids with Slower-Response Resources

This section presents the requirements and specifications associated with APR of GFM PV plants in a mixed-source microgrid (i.e., with slower-response resources such as synchronous generators). In this scenario, the APR can be provided by the synchronous generators or the GFM PV plants, or both. However, as discussed in chapter 3, the slower governor response can cause issues if the APR is solely provided by synchronous generator (SG), which necessitates up-reserves from GFM PV plants.

Steady state requirements

Compared with fast-responding inverters, the governor response of a SG is slow. As a result, it picks up the load after a load increase in a much slower rate. In a microgrid with high PV penetration, the inertia level of the system is low. This coupled with the slower governor response of SG can result in large frequency drop following a load increase, if the power reserve is provided only by the SG. To avoid this, PV plants should provide up-reserves and help pick up a portion of the load following a load increase.

A method to set the droop curves of the PV and the SG P-f functions to achieve this is shown in Figure 24. This setting approach guarantees that there is sufficient headroom from the PV plant even when the available power is at the minimum estimated value. Notice that this method again assumes that PV and load forecast is available to the microgrid controller and the

microgrid controller can dispatch the PV and SG plant droop curve periodically. To ensure that the dynamic frequency following a worst-case load disturbance is bounded within an acceptable frequency range, the slope of the SG and PV droop slopes should be properly designed. Two ways to design the droops slopes will be discussed in the following sections.

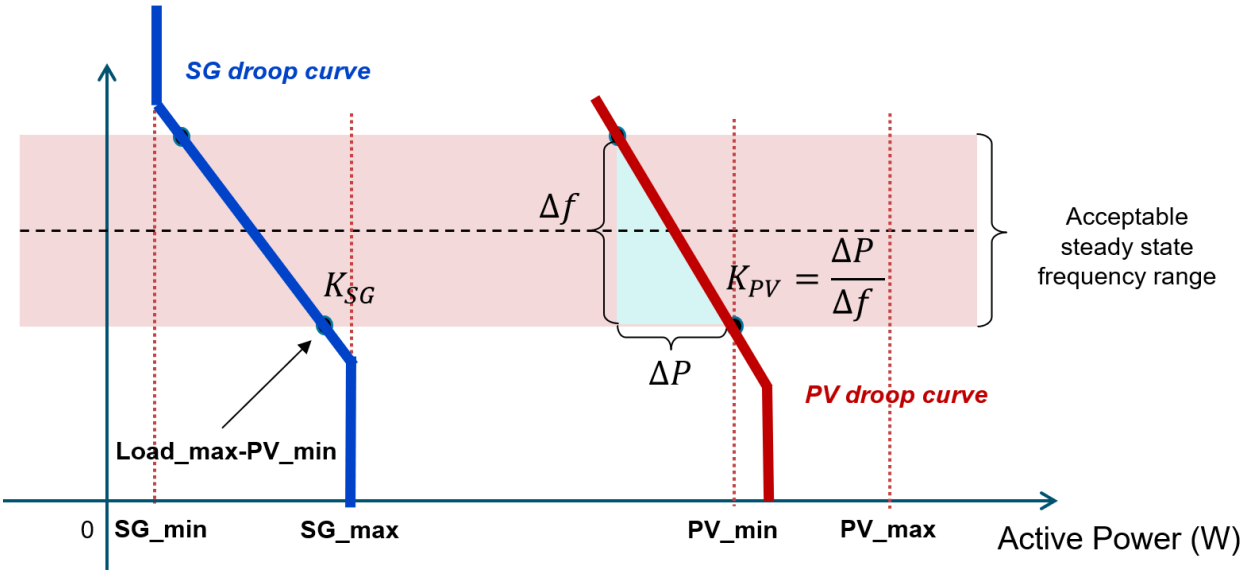


Figure 24. The proposed P-f droop setting approach for PV and SG plants

Dynamic/transient requirements

In designing the steady state requirements with PV plants providing up-reserves to help microgrid frequency, it is again assumed that PV plants act much faster than SGs. As discussed in the previous section, even though inverter-based plants are able to respond fast, without explicit requirements, the dynamic response of the plants may not be sufficient to maintain stability and acceptable frequency dynamics following a load disturbance. Therefore, dynamic/transient requirements for GFM PV plants are required to ensure stable and acceptable frequency dynamics in the microgrid. A microgrid with multiple inverter-based GFM PV plants and a SG is considered and the requirements for each individual plant as well as a setting guideline considering the interaction between multiple GFM plants and the SG are developed.

Requirements on a single GFM plant

For a single GFM PV plant, the same requirement presented in the previous section can be applied here. The requirements ensures that each individual GFM PV plant is capable to limit the frequency deviation following a load disturbance and provide sufficient damping. These individual plant requirements help the entire microgrid frequency in a mixed-source microgrid, even though they cannot guarantee the performance of the microgrid frequency, which calls for a system level setting guideline to be described next.

Setting guideline considering the interaction between multiple GFM plants and SG

As mentioned, the individual plant requirements can improve the performance of the overall system, but they are no longer sufficient to guarantee acceptable frequency dynamics and stability considering the interaction between multiple plants. A setting guideline to set the droop slopes of the various GFM plants and the SG to ensure satisfactory frequency dynamics in the microgrid is necessary.

Reference model for the diesel generator frequency

To consider a diesel generator with P-f droop, we propose to use a second-order reference model that mimics a synchronous generator with speed droop governor, first-order turbine dynamics, turbine power limits, and ramp rate limits. This reference model is given by

$$M\,\frac{\mathrm{d}}{\mathrm{d}t}\omega_{ref} = sat_{P_{T,min}}^{P_{T,max}}(P_T) - P_e$$

$$\frac{\mathrm{d}}{\mathrm{d}t}P_T = sat_{R_{T,min}}^{R_{T,max}}\left(-\frac{1}{T_T}P_T - \frac{1}{T_T}K_{dr}\left(\omega_{ref} - \omega_0\right)\right)$$

Where M denotes the diesel generator inertia constant in seconds, $P_{T,max}$ and $P_{T,min}$ denote the turbine power limits in system base, K_{dr} denotes the speed droop gain of the reference model in system base, and $R_{T,max}$ and $R_{T,min}$ denote the normalized turbine ramp rate limits in system base, and T_T denotes the time constant of the (virtual) reference turbine dynamics in seconds. We emphasize that the inertia constant M, power limits, and ramp rate limits should approximately correspond to the inertia and limits of the diesel generator. Moreover, T_T should be selected to approximate the response time of the diesel governor. We assume that the parameters can be approximated based on the results of a few experiments (e.g., load steps of varying size) performed on the actual diesel generator.

This approach allows us to approximate the complex closed-loop diesel generator frequency dynamics with the simple second-order reference model for analysis purposes as discussed next.

Microgrid frequency dynamics

We consider grid-forming PV inverters that implement standard droop control

$$\omega_k - \omega_0 = m_{p,k}(P_k^* - P_k)$$

with frequency droop coefficient $m_{p,k}$, power setpoint P_k^* and inverter active power injection P_k. For typical diesel generators, the frequency response of the diesel generator in closed loop with the second-order reference dynamics are significantly slower than the response of the inverters and network circuit dynamics. This motivates the use of an aggregate model that maps the fast inverter response to the diesel generator bus and neglects the fast dynamic interactions between the inverters. In this setting, the inverter dynamics as seen from the

diesel generator can be modeled by an equivalent turbine with effective time constant $T_{c,k} = 1/b_k m_{p,k}$ that depends on the droop coefficient $m_{p,k}$ and susceptance b_k between the inverter with index k and the diesel generator[8].

Frequency dynamics at the diesel generator bus

Explicit analytical expressions for the frequency nadir of this model are generally too complicated to be of use. Instead, if the ramp rate and turbine limits are significant one needs to resort to simulation studies to find suitable droop coefficients. In the remainder, we assume that that the turbine limits are only active for short periods of time during normal operation and use the small-signal model where all signals are deviations from the nominal operating point.

$$M \frac{\mathrm{d}}{\mathrm{d}t} \Delta\omega_{ref} = \Delta P_T - \Delta P_l + \sum_{k=1}^{N} \Delta P_{c,k}$$

$$T_T \frac{\mathrm{d}}{\mathrm{d}t} \Delta P_T = -P_T - K_{dr}\, \Delta\omega_{ref}$$

$$T_{c,k} \frac{\mathrm{d}}{\mathrm{d}t} \Delta P_{c,k} = -\Delta P_{c,k} - m_{p,k}^{-1}\, \Delta\omega_{ref}$$

We first note that the steady-state frequency deviation of this model is given by $\Delta\omega_s = 1/(K_{dr} + \sum_{k=1}^{N} m_{p,k}^{-1})\, \Delta P_l$, which can be tuned through $m_{p,k}$ and K_{dr}. However, in this case, the frequency also exhibits a frequency nadir, i.e., after a load step the frequency reaches a minimum before it increases and converges to the steady-state frequency $\Delta\omega_s$.

To analyze the frequency nadir and damping of the frequency dynamics, further model reduction is required. To this end, we note that for typical parameter values it holds that $T_{c,k} \ll T_T$. This motivates two approximations. Replacing the turbine and inverter dynamics by their dominant pole at $1/T_T$ results in the model

$$M \frac{\mathrm{d}}{\mathrm{d}t} \Delta\omega_{ref} = \Delta P_a - \Delta P_l$$

$$T_T \frac{\mathrm{d}}{\mathrm{d}t} \Delta P_a = -P_T - \left(K_{dr} + \sum_{k=1}^{N} m_{p,k}^{-1}\right) \Delta\omega_{ref}$$

that will overestimate the maximum frequency deviation (i.e., nadir) of diesel generator.

Specifically, the corner frequency ω_c and damping ratio ξ of the poles of the dominant pole approximation of the diesel generator dynamics are given by

[8] B. K. Poolla, Y. Lin, A. Bernstein, E. Mallada and D. Groß, "Frequency Shaping Control for Weakly-Coupled Grid-Forming IBRs," in *IEEE Control Systems Letters*, vol. 7, pp. 937-942, 2023

$$\omega_c = \sqrt{\frac{\sum_{k=1}^{N} m_{p,k}^{-1} + K_{dr}}{MT_T}}, \xi = \frac{M}{\sqrt{MT_T\left(\sum_{k=1}^{N} m_{p,k}^{-1} + K_{dr}\right)}}$$

Thus, decreasing the droop coefficients directly improves the damping ratio and increases the resonance frequency of the aggregate frequency dynamics.

To analyze the frequency nadir, we note that the nadir (i.e., minimum frequency after a load step) is not affected by rescaling the time axis. Rescaling time in the aggregate frequency dynamics by the turbine time constant T_T results in

$$\frac{M}{T_T}\frac{\mathrm{d}}{\mathrm{d}t'}\Delta\omega_{ref} = \Delta P_a - \Delta P_l$$

$$\frac{\mathrm{d}}{\mathrm{d}t'}\Delta P_a = -P_T - \left(K_{dr} + \sum_{k=1}^{N} m_{p,k}^{-1}\right)\Delta\omega_{ref}$$

Consequently, given M/T_T, the frequency nadir can be directly computed for a range of effective droop gains $K_{dr} + \sum_{k=1}^{N} m_{p,k}^{-1}$ (see Figure 25).

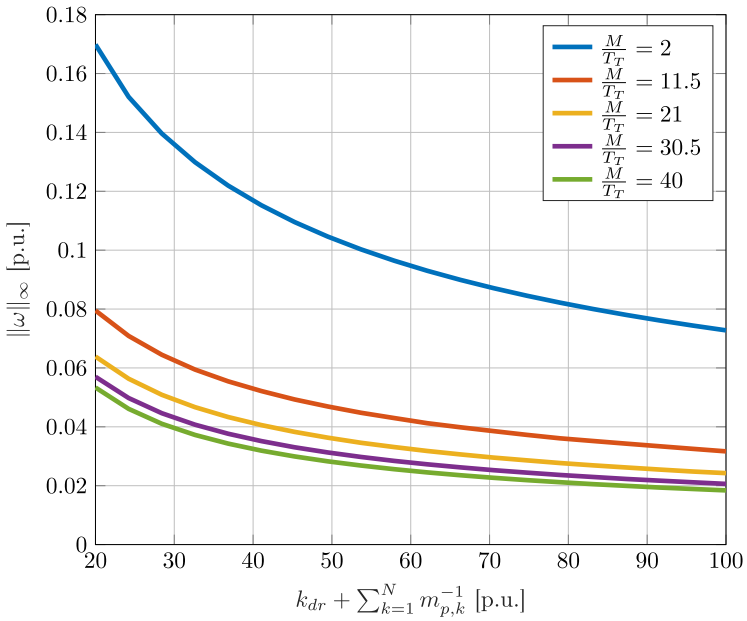


Figure 25. Frequency nadir for various M/T_T ratios and effective droop gains $K_{dr} + \sum_{k=1}^{N} m_{p,k}^{-1}$ for a 1 p.u. load step

Average inverter frequency dynamics

Assuming strong coupling (i.e., small line impedances) and repeating the same procedure to map the diesel generator frequency response to the average inverter frequency dynamics results in the model

$$\frac{M}{T_T}\frac{\mathrm{d}}{\mathrm{d}t'}\Delta\omega_{IBR} = \Delta P_a - \Delta P_l + \sum_{k=1}^{N} m_{p,k}^{-1}\Delta\omega_{IBR}$$

$$\frac{\mathrm{d}}{\mathrm{d}t'}\Delta P_a = -P_T - K_{dr}\Delta\omega_{IBR}$$

That approximates the average inverter frequency dynamics for a load step at an inverter bus. The corner frequency ω_c and damping ratio ξ of the poles of the aggregate frequency dynamics (with respect to the original time t) are given by

$$\omega_c = \sqrt{\frac{\sum_{k=1}^{N} m_{p,k}^{-1} + K_{dr}}{MT_T}}, \xi = \frac{M + T_T\sum_{k=1}^{N} m_{p,k}^{-1}}{\sqrt{MT_T\left(\sum_{k=1}^{N} m_{p,k}^{-1} + K_{dr}\right)}}$$

Thus, in comparison to the dominant pole approximation of the frequency dynamics at the diesel generator bus, a more significant increase of the frequency damping at the inverter buses is predicted for a decrease in inverter frequency droop coefficient.

Assuming a fixed ratio M/T_T, the frequency nadir for a range of (reference) governor gains K_{dr} and aggregate inverter droop gains $\sum_{k=1}^{N} m_{p,k}^{-1}$. Figure 26 shows a plot of the frequency nadir for $M/T_T = 10$ (e.g., one second of inertia and a turbine time constant of 100 ms) and a parameter sweep over K_{dr} and $\sum_{k=1}^{N} m_{p,k}^{-1}$.

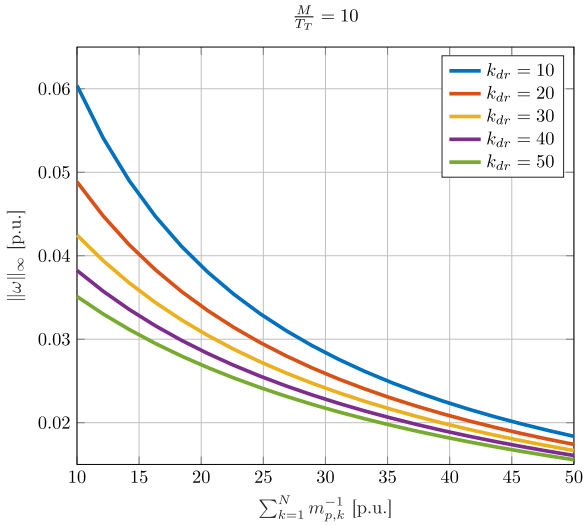


Figure 26. Frequency nadir for different (reference) governor gains K_{dr}, aggregate inverter droop gains $\sum_{k=1}^{N} m_{p,k}^{-1}$, and $M/T_T = 10$

Setting guidelines to limit the overall frequency deviation

Given a maximum load deviation, Figure 25 and Figure 26 can be directly created for the given diesel generator parameters to select droop gains that limit the frequency deviation at the

diesel generator and average inverter frequency deviation, which serves as the first method to set the droop slopes in Figure 24.

Note that this method assumes that the GFM PV inverter is based on Droop Control and the diesel generator can be effectively approximated by a second-order reference model that mimics a SG with speed droop governor and first-order turbine dynamics. Moreover, the approximations used to derive the bounds are typically justified for systems with strong coupling. The method becomes less accurate when these assumptions are not justified, which motivates a simulation-based P-f droop setting guideline to be presented next.

Simulation-based setting guideline and demonstration

This section presents simulation results that demonstrate the effectiveness of the droop setting approach shown in Figure 24, together with the simulation-based method to set the P-f droop slopes for GFM PV and SG.

The same modified IEEE 13 bus feeder shown in Figure 14 is considered as an example mixed-source microgrid with high PV penetration. The total capacity from PV is 4MW which is around 86% of the total generation capacity inside the microgrid.

Case study A: simulation-based method to determine the droop slopes

Since the previous analytical method to determine the droop slopes involves assumptions and approximations which may not hold true for all the scenarios, in this section, a simulation-based method is proposed as an alternative approach. Since the droop slopes are obtained based on simulation studies, it does not include approximations. However, it requires accurate dynamic simulation models that faithfully represents the behavior of both the SG and the PV GFM plants. Given that such models are available, simulation studies with the worst-case planned load disturbance can be conducted with different slope settings to identify the range of settings that results in satisfactory frequency performance.

Assume that the worst-case load increase that the microgrid is planned for is 10% of peak load, which is around 400 kW. A series of simulation studies can be done starting from PV plants not providing up reserve (i.e., working at MPP). The results for this scenario are shown in Figure 27 as Case 1. As can be seen, following the load increase at 7.5s, the PV plant only increases its output momentarily then settles to the MPP at 1500kW. The SG picks up the entire 400kW load. As a result, the frequency dips to around 58Hz.

The droop slope of the PV is then gradually increased. As another scenario, the PV droop slope is set such that the PV plant will pick up 200kW following the load step increase, as shown in Figure 27 (Case 2). Because of the faster active power response from PV, the frequency dip in this scenario is around 58.75 Hz. Suppose the acceptable frequency nadir is above 58.5 Hz, the PV droop slope in this scenario can be used as a lower limit. In other words, when setting the droop slope for PV according to Figure 24, it should not be below the value identified in Case 2. Note having a greater PV droop slope (K_{pv}) can regulate the frequency tighter and further

improve the frequency response. However, it at the same time requires more up-reserve from the PV plant, which is not economic as the PV needs to curtail further and the SG needs to burn more fuel. Therefore, the PV droop slope should be set close to the limit identified whenever possible.

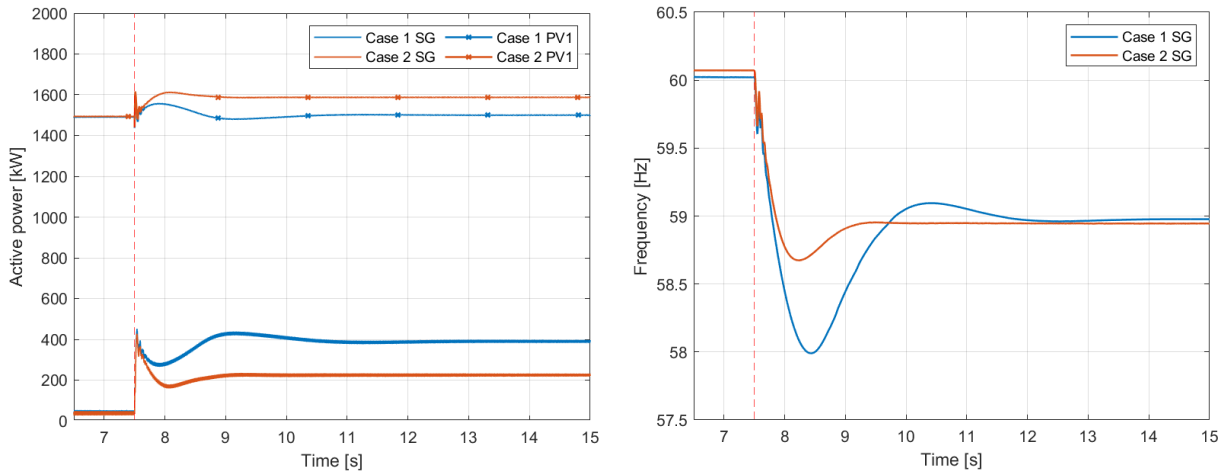


Figure 27. Illustration of the simulation-based slope setting approach

Moreover, both the SG and the PV plant droop slope affect the frequency nadir while the PV droop has more impact in general. Therefore, instead of searching for both SG and PV droop slopes, the SG droop slope can be fixed at the highest value allowed by the SG (e.g., 2%) while searching for the lowest PV droop slope without violating the nadir requirement.

Case study B: 10% load increase in two steps

The droop setting approach is based on worst case load disturbance, which should also ensure that the frequency dip is well constrained with consecutive smaller load step changes, even though each smaller load step change would "consume" some of the up-reserve from the PV plant. To verify this, a case study is constructed where the 10% load increase is applied in two even steps (5% each time) and the results are shown in Figure 28. Case 2 in the figure is the same as the Case 2 in Figure 27 where the 10% load step increase is applied in one step. In comparison, when the load increase is applied in two even steps, the frequency dip is smaller, which is as expected, and it demonstrates the effectiveness of the setting approach in dealing with smaller consecutive disturbances.

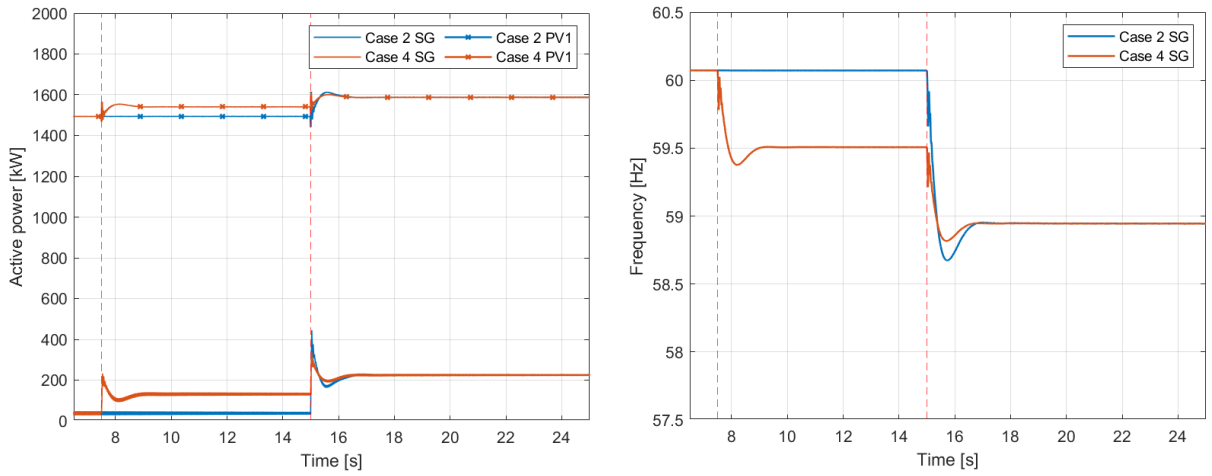


Figure 28. Verification of the droop setting approach with consecutive load changes

Case study C: change in initial operating condition

In practice, the worst-case load disturbance may occur at different system loading conditions. In this case study, the droop setting approach is verified at the different initial operating condition where the SG is generating more power. The results are shown in Figure 29. Again Case 2 corresponds to the case presented in case studies A and B. In comparison, Case 5 is the new case where the SG shares more load initially. Following the disturbance, the same droop slope setting results in the same increase in PV and SG power in both cases. Moreover, from the frequency plot, it can be seen that the nadir is very similar which indicates that the droop settings obtained based on studies in one loading scenario can be applied to other loading scenarios.

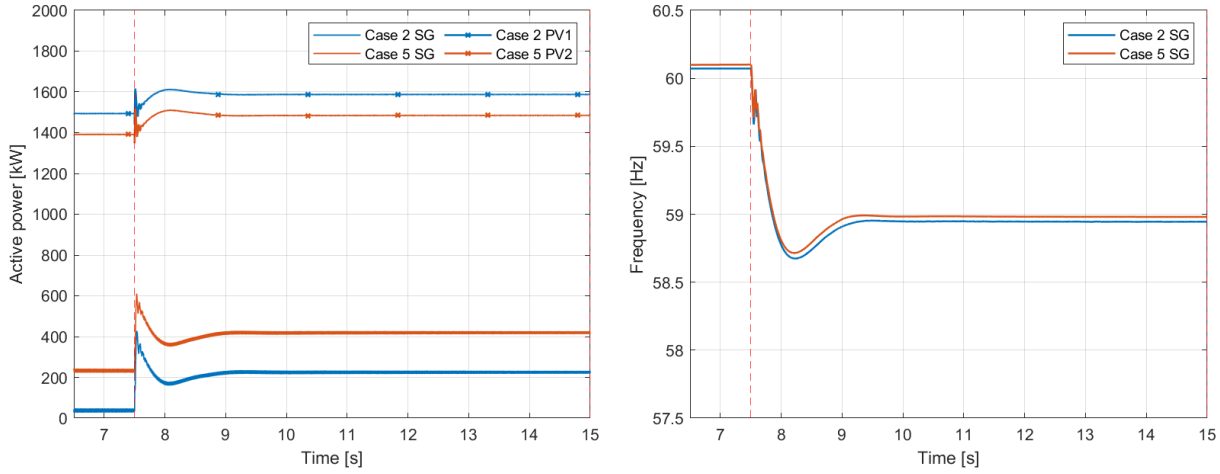


Figure 29. Verification of the droop setting approach with change in initial operating condition

5 STABILITY ANALYSIS IN MICROGRIDS WITH GFM PV AND DIESEL GENERATOR

In chapter 4, the P-f droop settings for GFM DERs (BESS, PV, and diesel generator) are designed with the goal to limit the frequency nadir and improve frequency dynamics in a microgrid. Another important aspect to consider when designing GFM DER settings is to maintain stability of the microgrid.

This chapter considers the mixed-source microgrid in Figure 14 with GFM PV and diesel generator and analyze the possible instability that may occur due to the interaction of multiple GFM DERs. The focus of this investigation is to study the impact of GFM DER voltage and frequency droop settings, diesel generator power limits, and GFM PV dc voltage control on the stability of the microgrid. Extensive numerical simulation studies have been conducted where a 10% load step change is considered. A screening tool has been developed that automatically screens various scenarios with different control gains, solar irradiation, and load for unstable dynamic interactions. In addition, methods to prevent the identified instability are discussed.

Stability Criteria

The stability of the microgrid is evaluated through measuring and then processing the voltage and frequency of the SG and GFM PV units. To this end, we first define the norm of the error (take frequency for example) before and after changing the system's loading condition as follows:

$$e_{f,1} = \|\omega_i - 60\|_2 \quad \text{for} \quad t < t_{cont}$$

$$e_{f,2} = \left\|\omega_i - \omega_{exp}\right\|_2 \quad \text{for} \quad t_{cont} < t$$

where t and t_{cont} are the simulation time and the time instant at which the system encounters an increase in the load. Before the load step, the frequency is expected to be around 60 Hz, so the error signal is obtained by comparing the system frequency to the nominal value. After the load change, the system frequency is supposed to converge to an expected value that can be obtained through the following equation in a system including N devices (e.g., SG and GFM PV):

$$\left|\omega^* - \omega_{exp}\right| = \Delta\omega^{syn} = \frac{1}{\sum_{i \in N} m_{p_i}^{-1}} \Delta P^{load}$$

where ω^* is the pre-disturbance frequency, ω_{exp} is the expected average frequency after the contingency, ΔP^{load} is the total deviation in the microgrid's loads (i.e., 10% or 0.1 p.u. in our scenarios), and $m_{p,i}$ is the droop percentage of the i-th unit. In a synchronized system, the frequency deviation for i-th device is equal to $\Delta\omega^{syn}$. Therefore, one has:

$$\Delta\omega^{syn} = \Delta\omega_i = m_{p_i}\Delta P_i$$

$$\sum_{i \in N} \Delta P_i = \Delta P^{load}$$

Here, ΔP_i is the deviation in the injected power by i-th device. By running a few simulation scenarios, one can select appropriate upper bounds for the error signals $e_{f,1}$ and $e_{f,2}$ to investigate small and large signal stability of the system. Let us consider the upper bounds to be δ_1 and δ_2, so the system is stable if both of the following conditions are met:

$$e_{f,1} < \delta_1$$

$$e_{f,2} < \delta_2$$

In fact, the first condition indicates small-signal stability, and the second one indicates large-signal stability. Therefore, the system needs to satisfy both conditions to remain stable. Similarly, the voltage deviation at each bus is monitored and evaluated.

Microgrid Stability with Different GFM PV and Diesel Generator Control Settings

Various control parameters may be adjusted to achieve a stable system. However, in a realistic setting most internal control parameters (e.g., inner loop gains, virtual impedance, internal filter time constants) are set by inverter manufacturer and cannot be tuned by microgrid operator. Therefore, we limit our investigation to parameters typically prescribed by system-level specifications (e.g., voltage and frequency droop settings). Overall, we assume that, for the SG, we can only change the frequency droop coefficient m_{sg}. On the other hand, for PVs, in addition to the voltage and frequency droop gains $m_{q,i}$ and $m_{p,i}$, we can set the lower dc voltage threshold for the dc voltage control embedded within the GFM PV system. Therefore, in total, we would have four parameters to tune and keep the system stable. In the following sections, the impact of these parameters on the system stability is identified and some suggestions are provided to keep the system stable.

Considerations in maintaining PV dc voltage stability

A typical P-V characteristic of PV panels is shown in Figure 5. As mentioned before, irrespective of the controls implemented, the PV system needs to remain in the stable region of the curve to maintain dc voltage stability. For single-stage PVs, providing active power droop and deviations from the initial power setpoint requires deviation from the nominal dc voltage to increase or decrease the PV's generated power. The sensitivity of the dc voltage deviation is defined by the curve's slope in the stable region. Note that decreasing the irradiance level decreases the MPP and the slope as well (see Figure 30). Linearizing PV's operating point in the stable region results in:

$$P_{pv,i} - P_{pv}^{*} = K_{pv,i}\left(V_{dc}^{*} - V_{dc,i}\right)$$

where $K_{pv,i}$ denotes the slope and determines the sensitivity of dc voltage deviation required for a fixed power deviation, $P_{pv,i}$ is the generated power by the PV, P_{pv}^* is the power setpoint, V_{dc}^* stands for the nominal dc voltage corresponding to the power setpoint, and $V_{dc,i}$ shows the new operating dc voltage associated with the power injected by the PV.

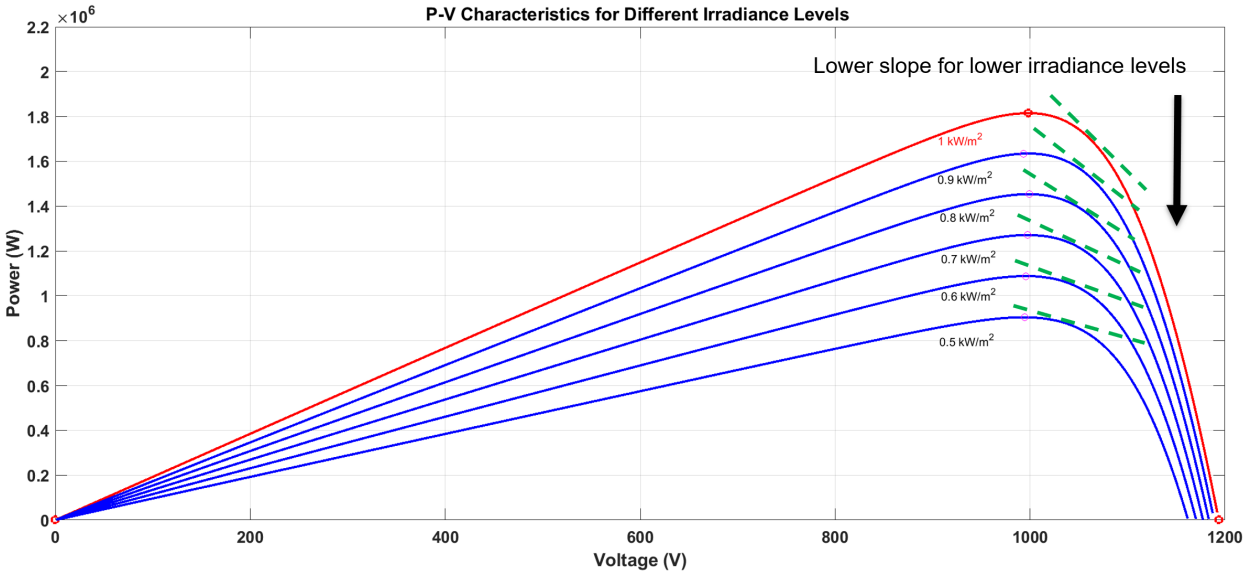


Figure 30. Example P-V characteristics for different levels of irradiance

To map this equation to the ac side, one can neglect power losses and substitute P_i for P_{pv}^* to obtain:

$$\omega_i - \omega^* = m_{p,i}\left(P_i^* - P_{pv}^* - K_{pv,i}\left(V_{dc}^* - V_{dc,i}\right)\right)$$

$$\omega_i - \omega^* = K_{pv,i} m_{p,i}\left(V_{dc,i} - V_{dc}^*\right)$$

Staying in the stable region imposes an upper limit on the dc voltage deviation. Moreover, given expected frequency deviations from the nominal value (i.e., a system-level protection design parameter) and maximum allowable dc voltage deviations (i.e., depending on the control and converter topology) results in the bounds

$$\left|V_{dc,i} - V_{dc}^*\right| \leq \Delta V_{max}$$

$$\left|\omega_i - \omega^*\right| \leq \Delta\omega_{max}$$

where ΔV_{max} and $\Delta\omega_{max}$ are the maximum allowable dc voltage and frequency deviations, respectively. Therefore, assuming that we have an estimate of the P-V characteristics and its slope for the next system-level dispatch interval, the following limit needs to be considered in choosing the ac side P-f droop $m_{p,i}$:

$$K_{pv,i} m_{p,i} \geq \frac{\Delta \omega_{max}}{\Delta V_{max}}$$

As can be seen from Figure 30, $K_{pv,i}$ reduces with lower irradiance. Therefore, $m_{p,i}$ should be set to higher values (regulating frequency less tightly) when irradiance reduces to maintain system stability. This point will be illustrated in the next section.

Stable regions in the parameter space

In this section, stability regions for different ranges of droop coefficients are presented. The screening tool automatically carries out simulations for various combinations of droop gains and assesses stability before and after the 10% load step change. Each point in Figure 31 corresponds to a simulated scenario for certain voltage and frequency droop coefficients. Blue dots correspond to stable cases. Magenta dots indicate the cases in which the PVs' dc voltage drops into the unstable region of the P-V curve. Red dots indicate cases in which the power generation of some, but not all, units saturate (usually PV units are saturated), i.e., some units do not follow their droop curve but at least one unit follows its droop curve. Finally, green dots correspond to scenarios where the power generation of all units saturates. To illustrating the results, the power setpoints of PV units and DG are 1740kW and 500kW. Furthermore, the irradiance level and the dc voltage threshold for these scenarios are 1000 $^{kW}/_{m^2}$ and 1020V, respectively. The system base power is 2 MW, where PVs and DG's capacities are 1.8 MW and 0.6 MW, respectively.

The result shown in Figure 31 is based on the 1%-20% device-based voltage and frequency droop range. Note 1% droop means that for 1% change in system frequency or voltage, the active or reactive power changes by 1pu. As can be seen, except for extreme voltage droop gains and a few specific droop combinations, the system remains stable.

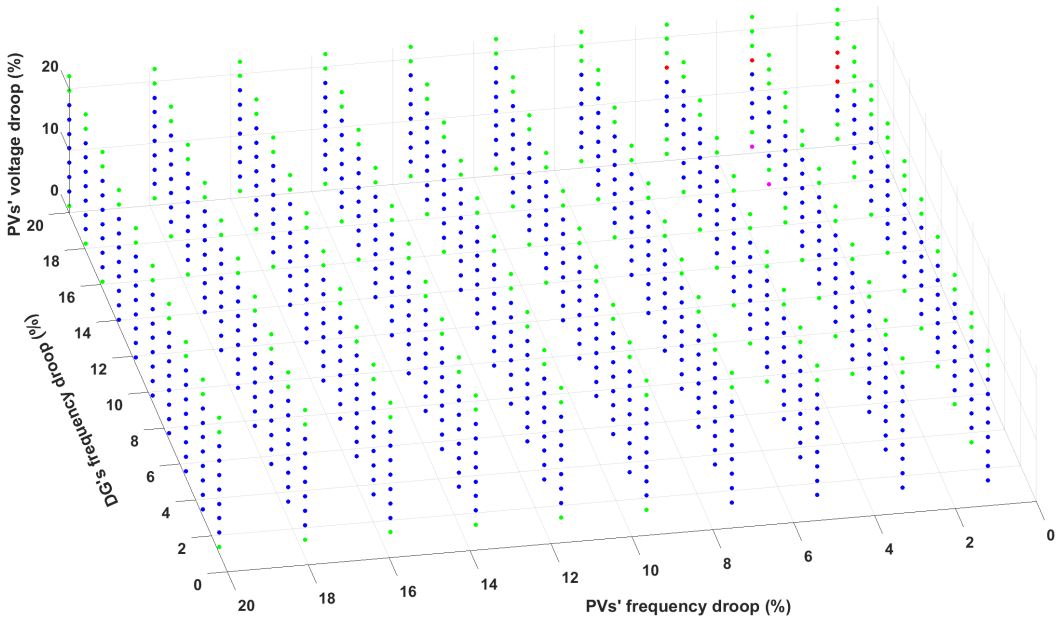


Figure 31. Stability regions for 1%-20% device based droop ranges

In the previous case, we assumed that the irradiance level was at its maximum value. Next, we explore the small- and large-signal stability boundaries of the system for lower irradiance levels. In this case, shown in Figure 32, the machine frequency droop is fixed at 7% and the PVs' voltage droop is fixed at 10%, and the PVs' frequency droop as well as dc voltage limit are varied for different levels of irradiance. Similar to the previous cases, blue points correspond to stable scenarios. Note that green and red dots in this case show small- and large-signal unstable scenarios, respectively. It can be seen that in scenarios with a lower level of irradiance, decreasing $m_{p,i}$ and increasing the dc controller voltage limit makes the system unstable.

In other words, instability is easier to occur when the solar irradiance is low, and setting GFM PV plant P-f droop gain less aggressive (e.g., 10% instead of 2%) and increasing the dc voltage limit of GFM PV dc voltage control can improve the microgrid stability.

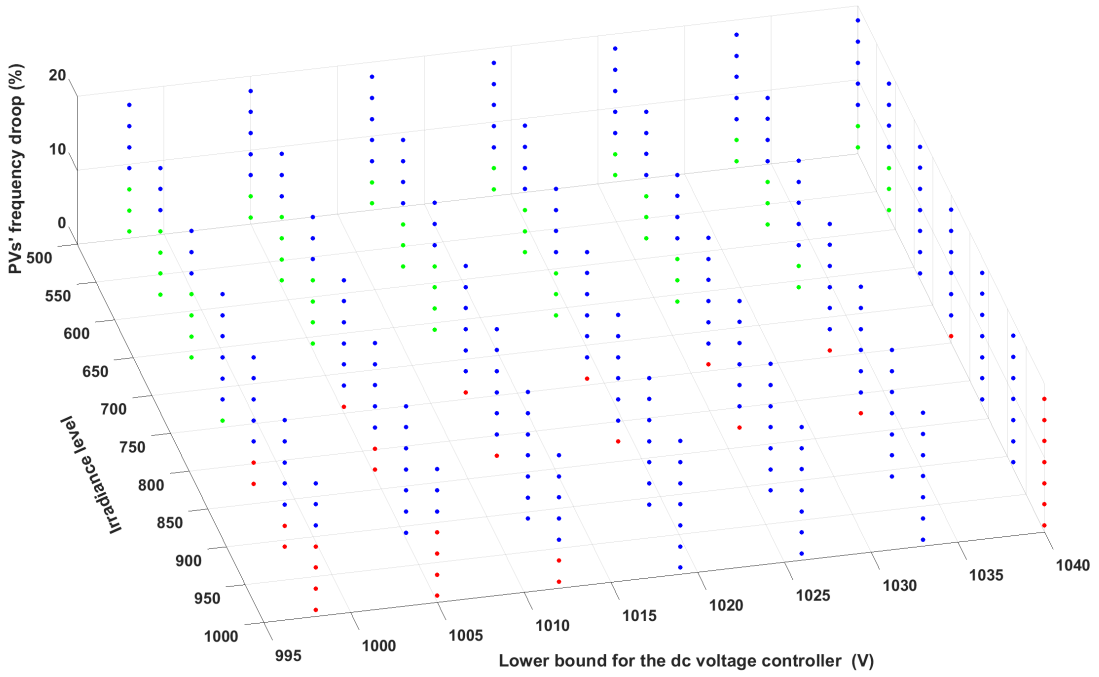


Figure 32. Stability regions for different levels of irradiance

Simulation Demonstration

Following the previous section, we next investigate the various unstable cases identified based on our stability criteria and identify the root causes of those instabilities. After conducting simulation studies for different loading conditions and various ranges of tunable parameters, the following observations were identified as the roots of the instability in the microgrid system:

- PV dc bus voltage drops into unstable region.
- All units reach their power limits and fail to serve the increased load.
- Low irradiance level

In the following, these root causes are discussed in more detail and illustrated using time-domain simulations as examples. In all scenarios, a load step change of 0.1 p.u. is applied at $t = 6s$.

PV dc bus voltage instability

As discussed above, the GFM PV units need to operate in the stable region of their P-V curve, independently of the controls they are using. As a result, once the operating point moves

toward the left side (i.e., lower dc voltage) and crosses the voltage corresponding to MPP, oscillations can be observed in the frequency and dc voltage waveforms. In many cases, the waveforms remain within a bounded region, but keep oscillating and do not converge to any steady state. These oscillations are the results of the dc voltage controller trying to keep the voltage greater than the MPP point and prevent the PV from entering the unstable region. Note that this is categorized as large-signal instability, given that a significant step load change is needed to perturb the operating point.

The root cause of this instability is the transient response of the dc voltage limiter. Specifically, dc voltage limiters for GFM control typically rely on proportional-integral (PI) control of the dc voltage through the ac side frequency that activates when the voltage reaches its limit. However due to the nature of the PI control response and ac network circuit dynamics the dc voltage typically undershoots lower dc voltage limits resulting in a limit cycle response. To resolve this issue without retuning the internal dc voltage limiter gains, we need to select the larger values as the lower bound of the dc voltage controller and smaller power setpoints such that PVs' operating points do not shift to the unstable region of the P-V curve. Moreover, picking small voltage droop gains can also amplify these oscillations and push the operating point to the left side. This type of instability does not depend on the system's available headroom and SG's setpoint. Ultimately, from a system-level perspective it needs to be ensured that transients and contingencies do not shift the operating point to the unstable region of the P-V curve. The simplest and most practical way to achieve this is to increase the lower dc voltage limit.

The following results show a scenario in which inappropriate selections of the lower bound for the dc voltage controller makes the system unstable after the contingency. As can be seen in Figure 33 and Figure 34, increasing the dc voltage limit from 1020V to 1040V makes the system stable. Note that the voltage plot in the figure is for the dc bus voltage. The increased dc voltage limit prevents the operating point from reaching or crossing the voltage corresponding to MPP, so the dc voltage remains in the stable region.

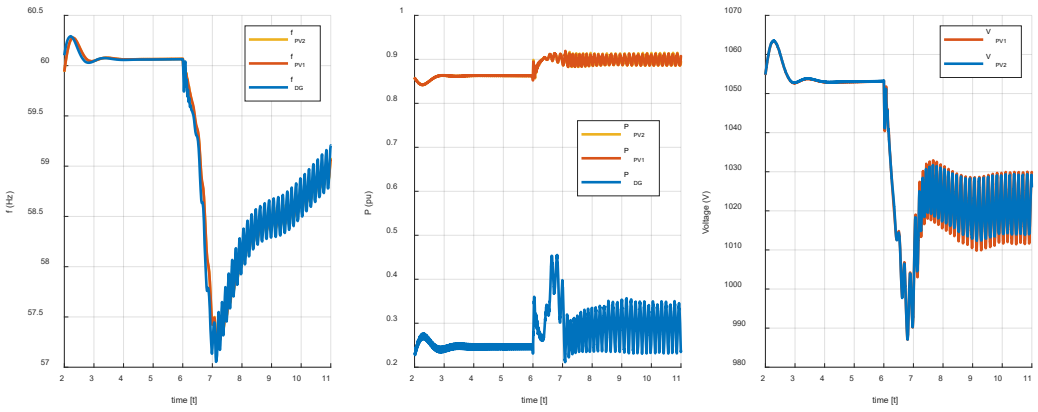


Figure 33. Instability caused by the dc voltage drop when the dc voltage limit is set to 1020V in the dc voltage controller

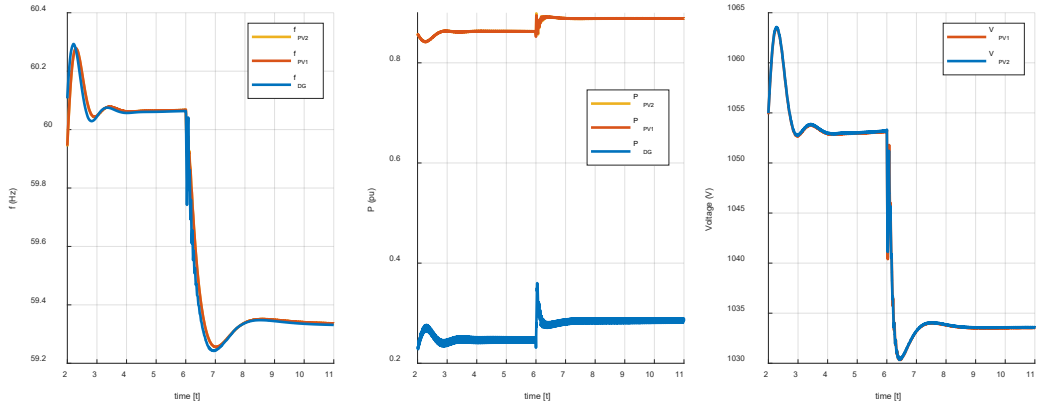


Figure 34. System recovered from dc voltage drop when the dc voltage limit is set to 1040V in the dc voltage controller

Instability caused by overloading the generation resources

When all units are injecting close to their maximum power, increasing the system's demand causes the units to saturate. Because of the resulting imbalance between supply and demand, the frequency collapses. If the saturation happens after changing the loading condition, the system's frequency does not converge to its steady-state and keeps dropping. This type of instability is directly related to the amount of available headroom and the loading condition of the microgrid.

To prevent this from happening, the power setpoints need to be adjusted carefully such that there is always enough headroom to supply additional loads during transients in case the system encounters such contingencies. When this cannot be achieved, proper load shedding mechanism should be implemented as the last resource. Another parameter that plays a vital role is voltage droop gain $m_{q,i}$. In some cases, increasing $m_{q,i}$ results in an increase system losses and results in overload of all units. For instance, the following results depicted in Figure 35 and Figure 36 represent a scenario in which increasing $m_{q,i}$ from 15% to 17% overloads all units. Usually, given fixed frequency droop gains, larger values of the voltage droop gain may result in saturation and instability. A preliminary recommendation is to decrease voltage droop gains and increase the headroom of the generation resources.

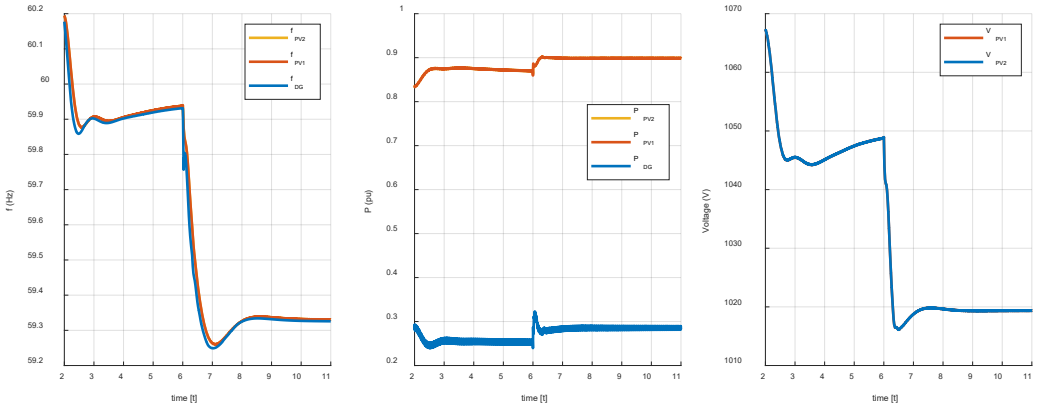


Figure 35. Stable system with sufficient headroom to cover load increase

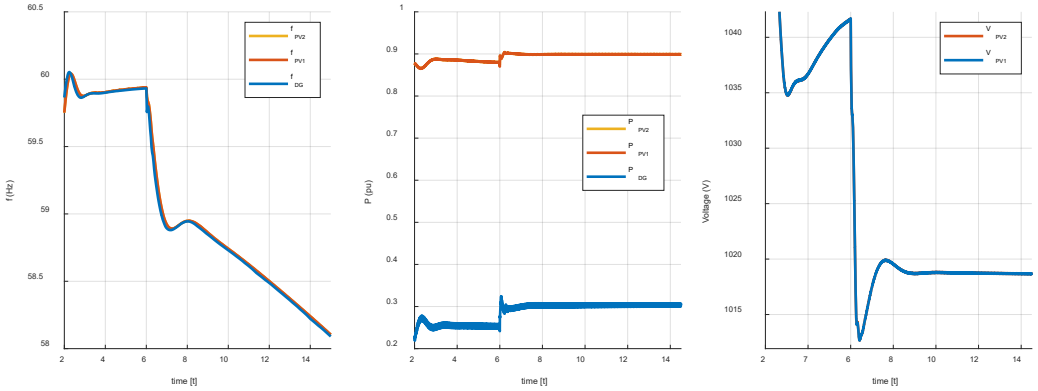


Figure 36. Instability caused by the saturation of all generation resources

Instability under low solar irradiance scenarios

In all previous cases, we assumed that the irradiance level for PVs is nominal. As irradiance constantly changes in practice, in this section, microgrid stability is investigated for different levels of irradiance. Our observations imply that both small-signal and large-signal instabilities become more likely with lower irradiance.

In the following, two numerical examples for the main instability mechanisms are discussed. Based on our observations, the two main factors affecting the stability in lower irradiance levels are (i) the dc voltage limit in GFM PV dc voltage control affecting the small-signal stability, and (ii) the PVs' frequency droop gain which impacts the large-signal stability.

Small signal instability

The simulation results depicted in Figure 37 illustrates a case in which reducing the lower dc voltage limit makes the system small-signal unstable. Note that it is classified as small-signal unstable since no large disturbance is applied in the system. The results are for the irradiance level of 666 $^{kW}/_{m^2}$. Keeping all the parameters and the loading condition the same but increasing the lower dc voltage limit from 1033V to 1040V makes the system stable. The results shown in Figure 38 correspond to the recovered system.

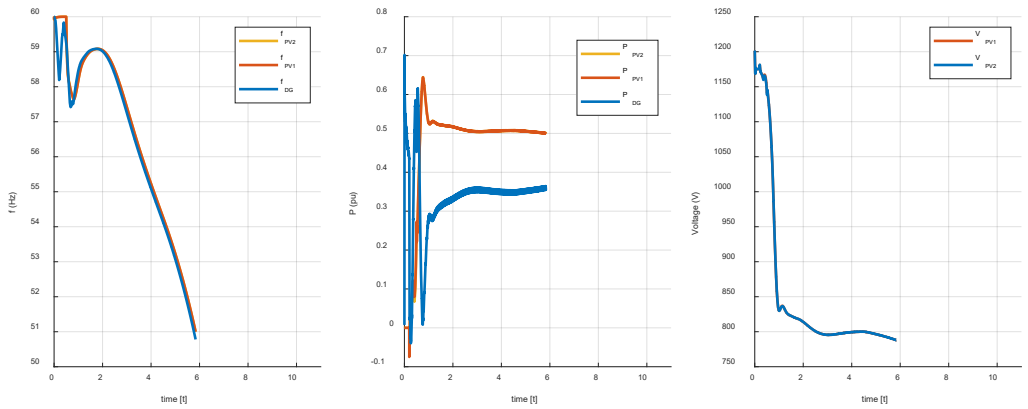


Figure 37. Small-signal instability caused by choosing inappropriate dc voltage limit

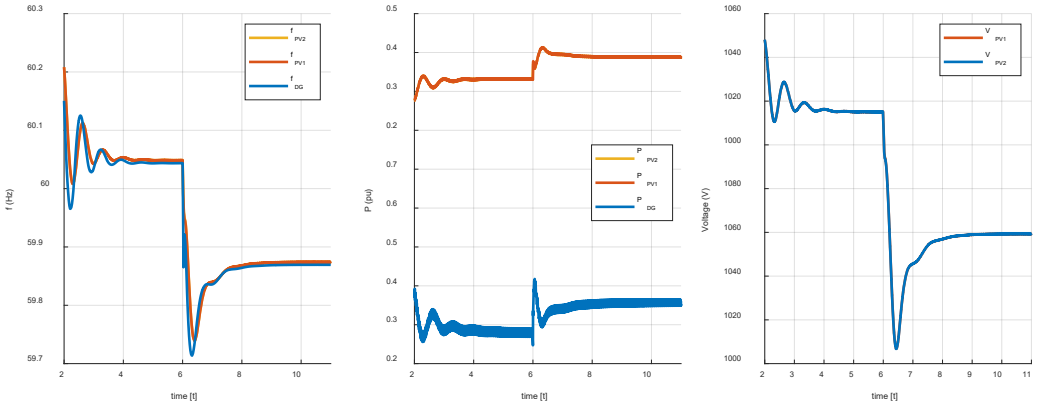


Figure 38. System recovered by increasing the dc voltage limit

Large signal instability

Large signal stability of the system is predominantly caused by aggressive GFM PV frequency droop settings. For low irradiance levels, choosing smaller droop constants puts more stress on PVs considering their lower maximum power. As a result, PVs cannot manage to supply the additional load after the contingency and their operating point shifts to the unstable region of the P-V curve. The results illustrated in Figure 39 and Figure 40 are related to a scenario in which increasing $m_{p,i}$ from 3.7% to 6% preserves the stability of the system. An example for

large-signal instability of the system is illustrated in Figure 39, where the frequency droop gain is set to be 3.7% and applying the load increase shifts the PVs operating point to the unstable region of the P-V curve. As a result of the instability, both PV dc bus voltage and the system frequency decrease.

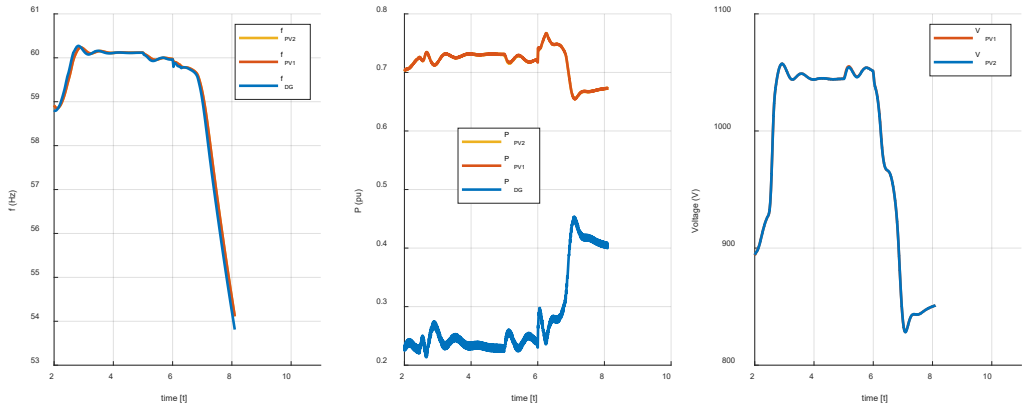


Figure 39. Large-signal instability caused by low frequency droop gain at low irradiance levels

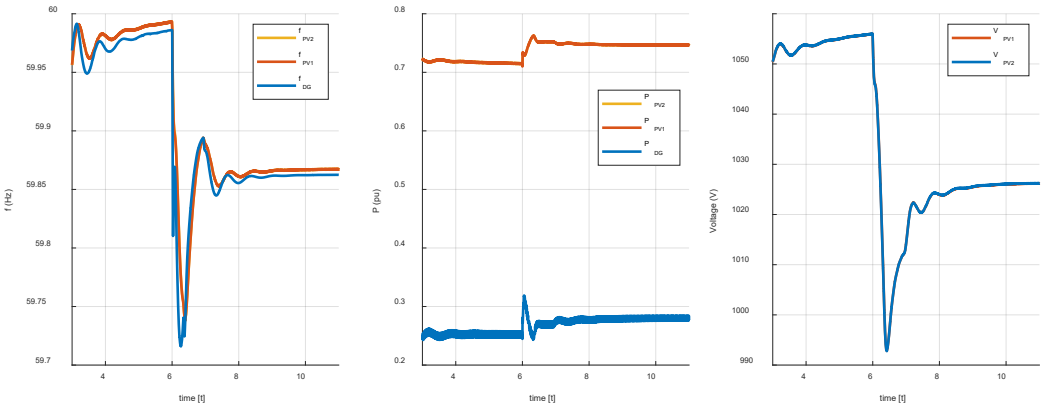


Figure 40. Stable system with high frequency droop gains at low irradiance levels

In summary, selecting larger values for the lower dc voltage limit in GFM PV control, avoiding small voltage droop constants, and lowering active power setpoints for PVs can prevent instability of the PV dc voltage that could propagate to the ac microgrid. This mechanism is not directly related to the amount of the system's headroom. The second instability mechanism, in which all generation resources saturate, can be avoided by increasing headroom, selecting reasonable voltage droop gains, and implementing proper load shedding scheme. The last instability mechanism occurs when GFM PVs are operating with a low irradiance level. In such cases, similar to the first mechanism, increasing the dc voltage controller limit and selecting larger frequency droop gains help keep the system stable.

6 CONCLUSION AND FUTURE WORK

This tech update presents results from the ongoing DOE SECURE project related to GFM PV inverter development and its application in utility-level microgrids. A particular design approach is illustrated and the control logics to limit the GFM PV plant active power output, stabilize dc voltage, and achieve active power up-reserve are presented in detail.

Even though active power up-reserve can be provided with the developed control design, it is demonstrated that in a fully inverter-based microgrid with GFM PV and GFM BESS, it could be beneficial to operate the GFM PV at maximum power point whenever possible while having the GFM BESS provide up-reserve. On the other hand, in mixed-source microgrids with GFM PV and diesel generator, due to the relative slower active power response rate of the diesel generator, up-reserve from GFM PV plants can significantly benefit the frequency stability of the microgrid.

Two methods to realize active power reserve from GFM PV plants are illustrated and the one that can be leveraged during dynamics as well as at steady state is implemented and discussed in detail. Performance requirements and specifications of the active power reserve function to realize the use cases are then presented, including steady state specification of the P-f droop settings and dynamic requirements to restrict frequency nadir.

Finally, stability of a microgrid with GFM PV and diesel generator reveals several potential instability risks caused by PV plant dc voltage instability, microgrid overloading, and low solar irradiance. Countermeasures are also discussed which include proper setting of the GFM PV dc voltage control parameters and the P-f droop settings.

EPRI is collaborating with Yaskawa Solectria Solar to implement the developed GFM PV control method on a commercial product and test it in the lab. Functions such as black start, frequency and voltage regulation, active power reserve will be tested and the results will be reported in future tech updates.

About EPRI

Founded in 1972, EPRI is the world's preeminent independent, non-profit energy research and development organization, with offices around the world. EPRI's trusted experts collaborate with more than 450 companies in 45 countries, driving innovation to ensure the public has clean, safe, reliable, affordable, and equitable access to electricity across the globe. Together, we are shaping the future of energy.

Program:

P174 DER Integration

3002028369

© 2023 Electric Power Research Institute (EPRI), Inc. All rights reserved. Electric Power Research Institute, EPRI, and TOGETHER…SHAPING THE FUTURE OF ENERGY are registered marks of the Electric Power Research Institute, Inc. in the U.S. and worldwide.

EPRI
3420 Hillview Avenue, Palo Alto, California 94304-1338 USA
800.313.3774 ▪ 650.855.2121 ▪ askepri@epri.com ▪ www.epri.com